University of Groningen

An adaptive multiscale hybrid-mixed method for the Oseen equations

Araya, Rodolfo; Cárcamo, Cristian; Poza, Abner H.; Valentin, Frédéric

Published in:
Advances in Computational Mathematics

DOI:
10.1007/s10444-020-09833-8

IMPORTANT NOTE: You are advised to consult the publisher's version (publisher's PDF) if you wish to cite from it. Please check the document version below.

Document Version
Publisher's PDF, also known as Version of record

Publication date:
2021

Link to publication in University of Groningen/UMCG research database

Citation for published version (APA):
Araya, R., Cárcamo, C., Poza, A. H., & Valentin, F. (2021). An adaptive multiscale hybrid-mixed method for the Oseen equations. *Advances in Computational Mathematics*, *47*(1), [15]. https://doi.org/10.1007/s10444-020-09833-8

Copyright
Other than for strictly personal use, it is not permitted to download or to forward/distribute the text or part of it without the consent of the author(s) and/or copyright holder(s), unless the work is under an open content license (like Creative Commons).

The publication may also be distributed here under the terms of Article 25fa of the Dutch Copyright Act, indicated by the “Taverne” license. More information can be found on the University of Groningen website: https://www.rug.nl/library/open-access/self-archiving-pure/taverne-amendment.

Take-down policy
If you believe that this document breaches copyright please contact us providing details, and we will remove access to the work immediately and investigate your claim.

Downloaded from the University of Groningen/UMCG research database (Pure): http://www.rug.nl/research/portal. For technical reasons the number of authors shown on this cover page is limited to 10 maximum.

Download date: 20-11-2022

Adv Comput Math (2021) 47: 15
https://doi.org/10.1007/s10444-020-09833-8

An adaptive multiscale hybrid-mixed method for the Oseen equations

Rodolfo Araya[1] · Cristian Cárcamo[1,2] · Abner H. Poza[3] · Frédéric Valentin[4]

Received: 19 December 2019 / Accepted: 15 December 2020 /
Published online: 2 February 2021
© The Author(s), under exclusive licence to Springer Science+Business Media, LLC part of Springer Nature 2021

Abstract

A novel residual a posteriori error estimator for the Oseen equations achieves efficiency and reliability by including multilevel contributions in its construction. Originates from the Multiscale Hybrid Mixed (MHM) method, the estimator combines residuals from the skeleton of the first-level partition of the domain, along with the contributions from element-wise approximations. The second-level estimator is local and infers the accuracy of multiscale basis computations as part of the MHM framework. Also, the face-degrees of freedom of the MHM method shape the estimator and induce a new face-adaptive procedure on the mesh's skeleton only. As a result, the approach avoids re-meshing the first-level partition, which makes the adaptive process affordable and straightforward on complex geometries. Several numerical tests assess theoretical results.

Communicated by: Paul Houston

✉ Abner H. Poza
apoza@ucsc.cl

Rodolfo Araya
rodolfo.araya@udec.cl

Cristian Cárcamo
ccarcamo@udec.cl

Frédéric Valentin
valentin@lncc.br

1 Departamento de Ingeniería Matemática & CI^{2}MA, Universidad de Concepción, Casilla 160-C, Concepción, Chile

2 Bernoulli Institute for Mathematics, Computer Science and Artificial Intelligence, University of Groningen, Groningen, The Netherlands

3 Departamento de Matemática y Física Aplicadas, Universidad Católica de la Santísima Concepción, Casilla 297, Concepción, Chile

4 Department of Mathematical and Computational Methods, LNCC - National Laboratory for Scientific Computing, Av. Getúlio Vargas, 333, Petrópolis, RJ 25651-070, Brazil

Keywords A posteriori error estimator · Oseen operator · Multiscale finite element · High-order approximation

Mathematics subject classification (2010) 65N12 · 65N15 · 65N30

1 Introduction

Fluid flow simulations rely on efficient numerical schemes shaped to account for large- and small-scale structures of the velocity and pressure fields. Typical problems are fluid flows in porous media and turbulent flows, for instance (for more details see [25, 32, 33, 50]). For those problems, the computational cost involving in numerical schemes that cope with small scales of the approximate solution is costly, especially when one considers time-dependent problems in three-dimensional geometries. For this reason, multiscale numerical methods have been attracted attention in the last decades by their "embarrassingly" parallel nature, which turn out to be an excellent option to leverage the new generation of massive high-performance computers.

The Multiscale Hybrid-Mixed (MHM) method is a member of the family of multiscale finite element methods. Multiscale methods have its origin in [13] for the one-dimensional Poisson problem, and they were further extended to higher dimensional cases in [42, 43]. Overall, the multiscale methods rely on incorporating fine scales of the solutions through basis functions, with an impact on the accuracy of coarse-scale solutions, which can be computed on a coarse partition with precision. Other members of this family are the Heterogeneous Multiscale method (HMM) [27], the Variational Multiscale method (VMS) [3], the Generalized Multiscale finite element method [28], the Localized Orthogonal Decomposition method (LOD) [40], the Petrov-Galerkin Enriched method (PGEM) [7, 16, 36], the Residual Local Projection method (RELP) [5, 17, 34], to mention a few. A posteriori error estimator for some of these schemes can be reviewed in [1, 10, 14, 21, 41, 44, 47, 49, 53], and the references therein.

Regarding the MHM method, it relies on the characterisation of the exact solution as a byproduct of the hybridisation of the continuous problem on a coarse mesh (first-level mesh). As a result, the exact fields decompose as the solutions of a series of local problems coupled through a global problem defined on the skeleton of the first-level partition. In such an infinite-dimensional setting, the local problems are entirely independent of one another and account for the multiscale nature of the problem. Discretisation uncouples global and local problems, and the latter responds for the multiscale basis computation. Thereby, the expensive part of the algorithm can be naturally solved in parallel computers. The MHM method was initially introduced for the Darcy equation in [38] and analysed in [8, 48], and extended to models based on the Stokes operator in [9] and [7].

In this work, we present a new MHM method for the Oseen equations, and propose and analyse a novel multiscale residual, a posteriori error estimator. The method combines the features of the MHM methods proposed in [39] and [11]. As for the estimator, it relies strongly on the MHM's structure, and as a result, the estimator splits into two levels: First η_1 accounts for the jump of the discrete velocity on the skeleton of the first-level mesh, and then, a second-level estimator η_2 estimates the error associated to the approximation of the local problems (multiscale basis, mostly). We prove local efficiency and reliability for the multiscale estimator following the ideas of [8, 11, 37] for η_1 and [11] for η_2. Besides, when we put the present work in the perspective of previous ones, it contributes to:

- propose the first MHM method for advective dominate flows with local mass preserving velocity field;
- present the first a posteriori error analysis for the MHM method applied to a non-symmetric operator. Note that [39] only provides a formal a posteriori error estimator for the one-level MHM method applied to the advective-reactive-diffusive equation;
- introduce a second-level a posteriori estimator η_2 which is also original. Indeed, only a priori error estimates have been proposed for the stabilised method [15] in the literature;
- extent the adaptive strategy on the mesh's skeleton proposed in [39]. Here, the strategy accounts for the interplay between the singular perturbed character of the model and its mixed form. As a result, the algorithm of adaption avoids re-meshing the first-level partition, which makes the adaptive process affordable to approximate boundary layered fluid flow problems on complex geometries.

Other numerical schemes share similarities with the MHM method but are also essentially different in their constructions and properties. For instance, we mention the Multiscale Mortar Method [12], the DEM [31], and the HDG method [24], for the Oseen equations [20], among others. For a small list of a posteriori error estimators for two-level method, see, for example, [18, 30, 45, 52, 54, 55] and the references therein.

The paper outlines as follows. In Section 2, we introduce the model problem, notations, and some preliminary results. Section 3 revisits the main aspects of the MHM methodology to propose new first- and second-level MHM methods for the Oseen equations. The main results of this work are in Section 4, wherein one proposes and analyses a new and multilevel a posteriori error estimator based on the MHM method. Numerical validations asses theoretical results in Section 5, and conclusions and perspectives lie in Section 6.

2 Model problem and preliminaries

2.1 The model

Let $\Omega \subset \mathbb{R}^d$, $d \in \{2, 3\}$, be a bounded open set with polygonal boundary $\partial\Omega$. Given $\boldsymbol{f} \in L^2(\Omega)^d$ and $\boldsymbol{g} \in H^{1/2}(\partial\Omega)^d$ with $\int_{\partial\Omega} \boldsymbol{g} \cdot \boldsymbol{n}\, ds = 0$, where $\boldsymbol{n}$ represents the outer normal vector to $\partial\Omega$, the Oseen problem consists of finding a velocity field $\boldsymbol{u}$ and scalar pressure p, such that:

$$\begin{aligned} -\nu\,\Delta\boldsymbol{u} + (\nabla\boldsymbol{u})\boldsymbol{\alpha} + \gamma\,\boldsymbol{u} + \nabla p &= \boldsymbol{f} \quad \text{in } \Omega, \\ \nabla\cdot\boldsymbol{u} &= 0 \quad \text{in } \Omega, \\ \boldsymbol{u} &= \boldsymbol{g} \quad \text{on } \partial\Omega, \end{aligned} \tag{1}$$

where the diffusion coefficient ν is a positive constant, $\boldsymbol{\alpha} \in W^{1,\infty}(\Omega)^d$ is a convective velocity field and γ a given scalar function. We assume in this work that γ is a positive constant and that there exists a positive constant γ_m such that, for all $x \in \Omega$, it holds:

$$\gamma_0 := \gamma - \frac{1}{2}\,\nabla\cdot\boldsymbol{\alpha}(\boldsymbol{x}) \geq \gamma_m. \tag{2}$$

Remark 1 Observe that model (1) may represent a step in the time discretisation of the unsteady Navier–Stokes equations, where $\gamma = 1/\Delta t$, with Δt the time interval length, and $\boldsymbol{\alpha}$ the velocity field evaluated in the previous time step (see, for example, [46]).

The standard variational mixed formulation associated to (1) reads: *Find $\boldsymbol{u} \in H^1(\Omega)^d$, with $\boldsymbol{u} = \boldsymbol{g}$ on $\partial\Omega$, and $p \in L^2_0(\Omega)$, such that:*

$$\begin{aligned} a(\boldsymbol{u},\boldsymbol{v}) + b(\boldsymbol{v},p) &= (\boldsymbol{f},\,\boldsymbol{v})_\Omega \qquad \text{for all } \boldsymbol{v} \in H^1_0(\Omega)^d, \\ b(\boldsymbol{u},q) &= 0 \qquad\qquad\quad \text{for all } q \in L^2_0(\Omega). \end{aligned} \tag{3}$$

The bilinear forms $a(\cdot,\cdot)$ and $b(\cdot,\cdot)$ are defined by:

$$a(\boldsymbol{w},\boldsymbol{v}) := \nu\,(\nabla\boldsymbol{w},\nabla\boldsymbol{v})_\Omega + ((\nabla\boldsymbol{w})\boldsymbol{\alpha},\boldsymbol{v})_\Omega + (\gamma\,\boldsymbol{w},\boldsymbol{v})_\Omega,$$

for all $\boldsymbol{w} \in H^1(\Omega)^d$, $\boldsymbol{v} \in H^1_0(\Omega)^d$ and:

$$b(\boldsymbol{v},q) := -(\nabla\cdot\boldsymbol{v},q)_\Omega,$$

for all $\boldsymbol{v} \in H^1(\Omega)^d$ and $q \in L^2_0(\Omega)$, where the spaces have their usual meaning. Using that:

$$((\nabla\boldsymbol{u})\boldsymbol{\alpha},\boldsymbol{v})_\Omega = -(\boldsymbol{u},(\nabla\boldsymbol{v})\boldsymbol{\alpha})_\Omega - ((\nabla\cdot\boldsymbol{\alpha})\boldsymbol{u},\boldsymbol{v})_\Omega + ((\boldsymbol{\alpha}\cdot\boldsymbol{n})\boldsymbol{u},\boldsymbol{v})_{\partial\Omega}, \tag{4}$$

for all $\boldsymbol{u},\boldsymbol{v} \in H^1(\Omega)^d$, follows that the bilinear form $a(\cdot,\cdot)$ can be rewritten in a skew-symmetry form as:

$$a(\boldsymbol{u},\boldsymbol{v}) := \nu\,(\nabla\boldsymbol{u},\nabla\boldsymbol{v})_\Omega + \frac{1}{2}\,((\nabla\boldsymbol{u})\boldsymbol{\alpha},\boldsymbol{v})_\Omega - \frac{1}{2}\,(\boldsymbol{u},(\nabla\boldsymbol{v})\boldsymbol{\alpha})_\Omega + (\gamma_0\,\boldsymbol{u},\boldsymbol{v})_\Omega\,,$$

for all $\boldsymbol{u} \in H^1(\Omega)^d$ and $\boldsymbol{v} \in H^1_0(\Omega)^d$.

Remark 2 Assumption (2) implies the coercivity of $a(\cdot,\cdot)$ in $H^1_0(\Omega)^d$, which combined with the classical inf–sup condition in $b(\cdot,\cdot)$, leads to the existence and unique solution for (3).

2.2 Hybridisation

Now we head to the definition of an equivalent hybrid form of (3). To this end, we introduce a regular family $\{\mathscr{T}_H\}_{H>0}$ of triangulations, in the sense of Ciarlet [22], of $\overline{\Omega}$, composed of simplexes K, with diameter H_K, and we set $H := \max\{H_K : K \in \mathscr{T}_H\}$. Hereafter, we shall use the terminology usually employed for three-dimensional domains, with the restriction to two-dimensional problems being straightforward. We denote by $\mathscr{E}_H$ the set of all faces (edges) F of elements $K \in \mathscr{T}_H$ and by $\mathscr{E}_0$ the set of inner faces. To each face F of $\mathscr{E}_H$, we associate a normal $\boldsymbol{n}$ taking care to ensure this is directed outward on $\partial\Omega$. For each $K \in \mathscr{T}_H$, we further denote by $\boldsymbol{n}^K$ the outward normal on ∂K, and let $\boldsymbol{n}_F^K := \boldsymbol{n}^K|_F$ for each $F \subset \partial K$. We denote by $\mathscr{T}_{\tilde{H}}(F)$ a partition of $F \in \mathscr{E}_H$, by $H_{\tilde{F}}$ the size of $\tilde{F} \in \mathscr{T}_{\tilde{H}}(F)$ and $\tilde{H} = \max\left\{H_{\tilde{F}} : \tilde{F} \in \mathscr{T}_{\tilde{H}}(F)\right\}$.

The following spaces will be used in the sequel:

$$\begin{aligned}
\mathbf{V} &:= H^1(\mathscr{T}_H)^d := \{\boldsymbol{v} \in L^2(\Omega)^d \ : \ \boldsymbol{v}|_K \in H^1(K)^d \quad \text{for all } K \in \mathscr{T}_H\}, \\
H(\mathrm{div};\Omega) &:= \{\boldsymbol{\tau} \in L^2(\Omega)^{d\times d} \ : \ \mathrm{div}\boldsymbol{\tau} \in L^2(\Omega)^d\}, \\
\boldsymbol{\Lambda} &:= \left\{\boldsymbol{\sigma}\, \boldsymbol{n}^K|_{\partial K} \in H^{-1/2}(\partial K)^d \quad \text{for all } K \in \mathscr{T}_H \ : \ \boldsymbol{\sigma} \in H(\mathrm{div};\Omega)\right\}, \\
Q &:= L^2(\Omega).
\end{aligned}$$

We define an inner product on $\mathbf{V}$ by:

$$(\boldsymbol{u}, \boldsymbol{v})_{\mathbf{V}} := \frac{1}{d_\Omega^2}(\boldsymbol{u}, \boldsymbol{v})_\Omega + \sum_{K\in\mathscr{T}_H} (\nabla\boldsymbol{u}, \nabla\boldsymbol{v})_K \quad \text{for all } \boldsymbol{u},\ \boldsymbol{v} \in \mathbf{V},$$

where d_Ω is the diameter of Ω, $(\cdot,\cdot)_D$ the L^2 inner product in $L^2(D)$, $D \subset \Omega$. We equip the spaces $H(\mathrm{div};\Omega)$ and $\mathbf{V}$ with the following norms:

$$\|\boldsymbol{\sigma}\|_{\mathrm{div}} := \left\{\sum_{K\in\mathscr{T}_H}\left[\|\boldsymbol{\sigma}\|_{0,K}^2 + d_\Omega^2\,\|\nabla\cdot\boldsymbol{\sigma}\|_{0,K}^2\right]\right\}^{1/2} \quad \text{and} \quad \|\boldsymbol{v}\|_{\mathbf{V}} := (\boldsymbol{v}, \boldsymbol{v})_{\mathbf{V}}{}^{1/2},$$

respectively. For the space $\boldsymbol{\Lambda}$, we use the quotient norm, i.e.:

$$\|\boldsymbol{\mu}\|_{\boldsymbol{\Lambda}} := \inf_{\substack{\boldsymbol{\sigma}\in H(\mathrm{div};\Omega)\\ \boldsymbol{\sigma}\boldsymbol{n}^K=\boldsymbol{\mu} \text{ on } \partial K,\, K\in\mathscr{T}_H}} \|\boldsymbol{\sigma}\|_{\mathrm{div}}. \tag{5}$$

We denote by $(\cdot,\cdot)_{\mathscr{T}_H}$ and $(\cdot,\cdot)_{\partial\mathscr{T}_H}$ the following:

$$(\boldsymbol{w}, \boldsymbol{v})_{\mathscr{T}_H} := \sum_{K\in\mathscr{T}_H} (\boldsymbol{w}, \boldsymbol{v})_K \qquad \text{and} \qquad (\boldsymbol{\mu}, \boldsymbol{v})_{\partial\mathscr{T}_H} := \sum_{K\in\mathscr{T}_H} \langle\boldsymbol{\mu}, \boldsymbol{v}\rangle_{\partial K},$$

where $\boldsymbol{w}, \boldsymbol{v} \in \mathbf{V}$ and $\boldsymbol{\mu} \in \boldsymbol{\Lambda}$, and $\langle\cdot,\cdot\rangle_{\partial K}$ is the duality pair between $H^{-1/2}(\partial K)^d$ and $H^{1/2}(\partial K)^d$.

We recall from Lemma 8.3 in [8] that the norm (5) is equivalent to a dual norm, namely:

$$\frac{\sqrt{2}}{2}\,\|\boldsymbol{\mu}\|_\Lambda \leq \sup_{\boldsymbol{v}\in\mathbf{V}} \frac{(\boldsymbol{\mu}, \boldsymbol{v})_{\partial\mathscr{T}_H}}{\|\boldsymbol{v}\|_{\mathbf{V}}} \leq \|\boldsymbol{\mu}\|_{\boldsymbol{\Lambda}} \quad \text{for all } \boldsymbol{\mu} \in \boldsymbol{\Lambda}. \tag{6}$$

Above and hereafter, we lighten the notation and understand the supremum to be taken over sets excluding the zero function, even though this is not specifically indicated.

We introduce the norm $\|(\cdot,\cdot)\|_{\mathbf{V}\times Q}$ for the product space $\mathbf{V}\times Q$, by:

$$\|(\boldsymbol{v},q)\|_{\mathbf{V}\times Q} := \left\{\|\boldsymbol{v}\|_{\mathbf{V}}^2 + \|q\|_Q^2\right\}^{1/2},$$

with $\|q\|_Q := \|q\|_{0,\Omega}$. Finally, for each $K \in \mathscr{T}_H$, we define the local spaces $\mathbf{V}(K) := H^1(K)^d$ and $Q(K) := L^2(K)$, with the follows norms:

$$\begin{aligned}
\|\boldsymbol{v}\|_{\mathbf{V}(K)} &:= \left\{d_\Omega^{-2}\,\|\boldsymbol{v}\|_{0,K}^2 + \|\nabla\boldsymbol{v}\|_{0,K}^2\right\}^{1/2},\\
\|q\|_{Q(K)} &:= \|q\|_{0,K},\\
\|(\boldsymbol{v},q)\|_{\mathbf{V}(K)\times Q(K)} &:= \left\{\|\boldsymbol{v}\|_{\mathbf{V}(K)}^2 + \|q\|_{Q(K)}^2\right\}^{1/2},
\end{aligned}$$

for all $\boldsymbol{v} \in \mathbf{V}(K)$ and $q \in Q(K)$.

Now, we consider the definition for the jump through a face $F = \partial K_n \cap \partial K_m \in \mathscr{E}_0$ of a function $\boldsymbol{v} \in \mathbf{V}$ as follows:

$$[\![\boldsymbol{v}]\!] := \begin{cases} (\boldsymbol{v}|_{K_n})|_F - (\boldsymbol{v}|_{K_m})|_F & \text{if } n > m \\ (\boldsymbol{v}|_{K_m})|_F - (\boldsymbol{v}|_{K_n})|_F & \text{if } n < m. \end{cases}$$

We update the notation $a(\cdot,\cdot)$ and $b(\cdot,\cdot)$ by extending them to the space $\mathbf{V}$ as follows:

$$a(\boldsymbol{w},\boldsymbol{v}) := \sum_{K\in\mathscr{T}_H} a_K(\boldsymbol{w},\boldsymbol{v}),$$

with:

$$a_K(\boldsymbol{w},\boldsymbol{v}) := \nu\,(\nabla\boldsymbol{u},\nabla\boldsymbol{v})_K + \frac{1}{2}\,((\nabla\boldsymbol{u})\boldsymbol{\alpha},\boldsymbol{v})_K - \frac{1}{2}\,(\boldsymbol{u},(\nabla\boldsymbol{v})\boldsymbol{\alpha})_K + (\gamma_0\boldsymbol{u},\boldsymbol{v})_K\,, \quad (7)$$

and

$$b(\boldsymbol{v},q) := \sum_{K\in\mathscr{T}_H} b_K(\boldsymbol{v},q) \quad \text{with} \quad b_K(\boldsymbol{v},q) := -(\nabla\cdot\boldsymbol{v},q)_K,$$

for all $\boldsymbol{w},\ \boldsymbol{v} \in \mathbf{V}$, $q \in Q$.

We consider the following hybrid formulation of problem (3): *Find* $(\boldsymbol{u},p,\boldsymbol{\lambda},\rho) \in \mathbf{V}\times Q\times\boldsymbol{\Lambda}\times\mathbb{R}$ *such that:*

$$\begin{cases} a(\boldsymbol{u},\boldsymbol{v}) + b(\boldsymbol{v},p) + (\boldsymbol{\lambda},\boldsymbol{v})_{\partial\mathscr{T}_H} = (\boldsymbol{f},\ \boldsymbol{v})_{\mathscr{T}_H} & \text{for all } \boldsymbol{v}\in\mathbf{V},\\ b(\boldsymbol{u},q) + (\rho,q)_\Omega = 0 & \text{for all } q \in Q,\\ (\boldsymbol{\mu},\boldsymbol{u})_{\partial\mathscr{T}_H} = \langle\boldsymbol{\mu},\boldsymbol{g}\rangle_{\partial\Omega} & \text{for all } \boldsymbol{\mu}\in\boldsymbol{\Lambda},\\ (\xi,p)_\Omega = 0 & \text{for all } \xi\in\mathbb{R}. \end{cases} \quad (8)$$

In formulation (8), the velocity and pressure belong a priori to a larger space than the solutions of the original problem (3). Note that the third equation in (8) imposes $H^1(\Omega)$–conformity on the velocity, and the fourth the mean value of the pressure equal zero. Concerning the solvability of problem (8), we have the following result

Theorem 1 *The pair* $(\boldsymbol{u}, p) \in H^1(\Omega)^d \times L^2_0(\Omega)$, *with* $\boldsymbol{u} = \boldsymbol{g}$ on $\partial\Omega$, *is the unique solution of* (3) *if and only if* $(\boldsymbol{u}, p, \boldsymbol{\lambda}, \rho) \in \mathbf{V} \times Q \times \boldsymbol{\Lambda} \times \mathbb{R}$ *is the unique solution of* (8). *Moreover, it holds* $\rho = 0$ *and:*

$$\boldsymbol{\lambda} = \left((-\nu\nabla\boldsymbol{u} + p\,\mathbf{I})\,\boldsymbol{n}^K + \frac{1}{2}\,(\boldsymbol{u}\otimes\boldsymbol{\alpha})\,\boldsymbol{n}^K\right)\bigg|_{\partial K} \quad \text{for all } K \in \mathscr{T}_H, \tag{9}$$

where $\mathbf{I}$ *is the* $d \times d$ *identity tensor.*

Proof Let $(\boldsymbol{u}, p)$ be the solution of (3), and define the functional $\mathscr{F} : \mathbf{V} \longrightarrow \mathbb{R}$ by:

$$\mathscr{F}(\boldsymbol{v}) := (\boldsymbol{f}, \boldsymbol{v})_{\mathscr{T}_H} - \nu(\nabla\boldsymbol{u}, \nabla\boldsymbol{v})_{\mathscr{T}_H} - \frac{1}{2}((\nabla\boldsymbol{u})\boldsymbol{\alpha}, \boldsymbol{v})_{\mathscr{T}_H} + \frac{1}{2}(\boldsymbol{u}, (\nabla\boldsymbol{v})\boldsymbol{\alpha})_{\mathscr{T}_H} - (\gamma_0\boldsymbol{u}, \boldsymbol{v})_{\mathscr{T}_H} + (\nabla\cdot\boldsymbol{v}, p)_{\mathscr{T}_H},$$

for all $\boldsymbol{v} \in \mathbf{V}$. It is clear that $\mathscr{F}$ is continuous and vanishes on $H^1_0(\Omega)^d$. From Lemma 1 in [51], there exists a unique $\boldsymbol{\lambda} \in \boldsymbol{\Lambda}$ such that $\mathscr{F}(\boldsymbol{v}) = (\boldsymbol{\lambda}, \boldsymbol{v})_{\partial\mathscr{T}_H}$ for all $\boldsymbol{v} \in \mathbf{V}$; thus, the first equation in (8) holds. Now integrating by parts we get:

$$\begin{aligned}\sum_{K\in\mathscr{T}_H} (\boldsymbol{\lambda}, \boldsymbol{v})_{\partial K} &= \sum_{K\in\mathscr{T}_H} \left[(\boldsymbol{f}, \boldsymbol{v})_K - \nu\,(\nabla\boldsymbol{u}, \nabla\boldsymbol{v})_K - \frac{1}{2}((\nabla\boldsymbol{u})\boldsymbol{\alpha}, \boldsymbol{v})_K + \frac{1}{2}(\boldsymbol{u}, (\nabla\boldsymbol{v})\boldsymbol{\alpha})_K - (\gamma_0\boldsymbol{u}, \boldsymbol{v})_K + (\nabla\cdot\boldsymbol{v}, p)_K\right]\\ &= \sum_{K\in\mathscr{T}_H} ((-\nu\nabla\boldsymbol{u} + p\mathbf{I})\boldsymbol{n}^K + \frac{1}{2}(\boldsymbol{u}\otimes\boldsymbol{\alpha})\boldsymbol{n}^K, \boldsymbol{v})_{\partial K},\end{aligned}$$

for all $\boldsymbol{v} \in \mathbf{V}$, and then (9) holds.

On the other hand, since that $(\nabla\cdot\boldsymbol{u}, q)_{\mathscr{T}_H} = (\nabla\cdot\boldsymbol{u}, q)_\Omega = 0$ for all $q \in L^2_0(\Omega)$, Lemma 5 in [9] guarantees that there exists a unique $\rho \in \mathbb{R}$ such that $(\nabla\cdot\boldsymbol{u}, q)_{\mathscr{T}_H} = (\rho, q)_\Omega$ for all $q \in Q$ and so the second equation of (8) holds. Now, using Gauss's Theorem, we get:

$$\|\rho\|^2_{0,\Omega} = \sum_{K\in\mathscr{T}_H} (\boldsymbol{u}\cdot\boldsymbol{n}^K, \rho)_{\partial K} = (\boldsymbol{u}\cdot\boldsymbol{n}, \rho)_{\partial\Omega} = (\boldsymbol{g}\cdot\boldsymbol{n}, \rho)_{\partial\Omega}.$$

By the compatibility condition, we have that $(\boldsymbol{g}\cdot\boldsymbol{n}, \rho)_{\partial\Omega} = 0$ and then $\rho = 0$. Next, take $\boldsymbol{q} \in H(\text{div};\Omega)$, and define $\boldsymbol{\mu} = \boldsymbol{q}\boldsymbol{n}^K$ on ∂K for all $K \in \mathscr{T}_H$. Using integration by parts, we have:

$$\begin{aligned}(\boldsymbol{\mu}, \boldsymbol{u})_{\partial\mathscr{T}_H} &= \sum_{K\in\mathscr{T}_H} \langle\boldsymbol{q}\boldsymbol{n}^K, \boldsymbol{u}\rangle_{\partial K} = \sum_{K\in\mathscr{T}_H} ((\nabla\cdot\boldsymbol{q}, u)_K + (\boldsymbol{q}, \nabla u)_K)\\ &= (\nabla\cdot\boldsymbol{q}, u)_\Omega + (\boldsymbol{q}, \nabla u)_\Omega = \langle\boldsymbol{q}\boldsymbol{n}, \boldsymbol{u}\rangle_{\partial\Omega} = (\boldsymbol{\mu}, \boldsymbol{g})_{\partial\Omega},\end{aligned}$$

this prove the third equation of (8). The fourth equation is true since $p \in L^2_0(\Omega)$ and $\xi \in \mathbb{R}$. This way we conclude that $(\boldsymbol{u}, p, \boldsymbol{\lambda}, \rho) \in \mathbf{V} \times Q \times \boldsymbol{\Lambda} \times \mathbb{R}$ satisfies (8) with $\rho = 0$, and:

$$\boldsymbol{\lambda} = \left[(-\nu\nabla\boldsymbol{u} + p\,\mathbf{I})\,\boldsymbol{n}^K + \frac{1}{2}\,(\boldsymbol{u}\otimes\boldsymbol{\alpha})\,\boldsymbol{n}^K\right]\bigg|_{\partial K} \quad \text{for all } K \in \mathscr{T}_H.$$

Reciprocally, let $(\boldsymbol{u}, p, \boldsymbol{\lambda}, 0) \in \mathbf{V} \times Q \times \boldsymbol{\Lambda} \times \mathbb{R}$ the unique solution of (8). From the fourth equation of (8), we have that $p \in L^2_0(\Omega)$. Let $\boldsymbol{u}_{\boldsymbol{g}} \in H^1(\Omega)^d$ such that $\boldsymbol{u}_{\boldsymbol{g}} = \boldsymbol{g}$ on $\partial\Omega$. Then, $\boldsymbol{u} - \boldsymbol{u}_{\boldsymbol{g}} \in \mathbf{V}$ and using the third equation of (8), we have that

$(\boldsymbol{\mu}, \boldsymbol{u} - \boldsymbol{u_g})_{\partial \mathcal{T}_H} = 0$ for all $\boldsymbol{\mu} \in \boldsymbol{\Lambda}$. This way, from Lemma 1 in [51], $\boldsymbol{u} - \boldsymbol{u_g} \in H_0^1(\Omega)^d$ and then $\boldsymbol{u} \in H^1(\Omega)^d$ with $\boldsymbol{u} = \boldsymbol{g}$ on $\partial\Omega$. From the second equation of (8) and considering $q \in L_0^2(\Omega)$, we get $b(\boldsymbol{u}, q) = 0$. Finally, using Lemma 1 of [51] and the first equation of (8), we have that:

$$a(\boldsymbol{u}, \boldsymbol{v}) + b(\boldsymbol{v}, q) = (\boldsymbol{f}, \boldsymbol{v})_{\mathcal{T}_H},$$

for all $\boldsymbol{v} \in H_0^1(\Omega)^d$, where we used $(\boldsymbol{\lambda}, \boldsymbol{v})_{\partial \mathcal{T}_H} = 0$. Therefore, $(\boldsymbol{u}, p)$ solves (3). Uniqueness of (8) follows from the uniqueness of (3). □

2.3 Standard results at local level

For the discrete analysis, we select two local finite dimensional spaces $\mathbf{V}_h(K) \subset \mathbf{V}(K)$ and $Q_h(K) \subset Q(K)$, whose functions are defined over a shape–regular partition of K, denoted by $\left\{\mathcal{T}_h^K\right\}_{h>0}$, where h is the characteristic length of $\mathcal{T}_h^K$. Particularly, hereafter we adopt the following polynomial spaces:

$$\mathbf{V}_h(K) := \left\{\boldsymbol{v}_h \in \mathbf{V}(K) \;:\; \boldsymbol{v}_h|_\tau \in \mathbb{P}_k(\tau)^d \;\text{ for all } \tau \in \mathcal{T}_h^K\right\}, \tag{10}$$

and

$$Q_h(K) := \left\{q_h \in Q(K) \cap C^0(K) \;:\; q_h|_\tau \in \mathbb{P}_n(\tau) \text{ for all } \tau \in \mathcal{T}_h^K\right\}, \tag{11}$$

where $\mathbb{P}_s(\tau)$ is the space of polynomial functions in $\tau \in \mathcal{T}_h^K$, with total degree less than or equal to s, $s \geq 1$. Thus, we define the global finite dimensional spaces as:

$$\mathbf{V}_h := \bigoplus_{K \in \mathcal{T}_H} \mathbf{V}_h(K) \quad \text{and} \quad Q_h := \bigoplus_{K \in \mathcal{T}_H} Q_h(K).$$

The set of faces ζ of $\mathcal{T}_h^K$ is denoted by:

$$\mathcal{E}_h^K := \mathcal{E}_0^K \cup \mathcal{E}_b^K,$$

where $\mathcal{E}_0^K$ is the set of internal faces and $\mathcal{E}_b^K = \mathcal{E}_h^K \setminus \mathcal{E}_0^K$, i.e. $\mathcal{E}_b^K$ are the faces of $\tau \in \mathcal{T}_h^K$ which belong to ∂K. Also, for each $\tau \in \mathcal{T}_h^K$ and $\zeta \in \mathcal{E}_h^K$, we denote by $\mathcal{N}(\tau)$ the set of nodes of τ, $\mathcal{N}(\zeta)$ the set of nodes of ζ, $\mathcal{E}(\tau)$ the set of edges of τ and then we define:

$$\omega_\zeta := \bigcup_{\zeta \in \mathcal{E}(\tau')} \tau', \qquad \tilde{\omega}_\tau := \bigcup_{\mathcal{N}(\tau) \cap \mathcal{N}(\tau') \neq \phi} \tau', \qquad \tilde{\omega}_\zeta := \bigcup_{\mathcal{N}(\zeta) \cap \mathcal{N}(\tau') \neq \phi} \tau'.$$

In the rest of this work, we will use the following notation:

$$\begin{aligned} a \preceq b &\iff a \leq C\, b, \\ a \succeq b &\iff a \geq C\, b, \\ a \simeq b &\iff a \preceq b \text{ and } a \succeq b, \end{aligned}$$

where the positive constant C may dependent on the physical constants, the shape–regularity constant of the mesh and the polynomial degree, but is independent of any mesh size.

Also, we will use standard bubble functions and some of the results associated with them. We consider the case with $d = 3$, but the same kind of results are valid with $d = 2$.

For all $\tau \in \mathscr{T}_h^K$, we define the element bubble function b_τ^K by:

$$b_\tau^K := (d+1)^{d+1} \prod_{x \in \mathscr{N}(\tau)} \lambda_x,$$

where λ_x corresponds to the barycentric coordinates associated to node x. Let $\hat{\tau}$ be the standard reference element with vertices $\tilde{n}_1 = (1, 0, 0)$, $\tilde{n}_2 = (0, 1, 0)$, $\tilde{n}_3 = (0, 0, 1)$, and $\tilde{n}_4 = (0, 0, 0)$ and define the edge bubble function by:

$$b_{\hat{\zeta}}^{\hat{K}} = d^d \hat{\lambda}_1 \hat{\lambda}_2 \hat{\lambda}_4,$$

where $\hat{\zeta} := \{(\hat{x}, \hat{y}, 0) \in \mathbb{R}^d : 0 \le \hat{x} + \hat{y} \le 1,\ \hat{x} \in [0, 1]\}$. For $\zeta \in \mathscr{E}_H$, assume that $\omega_\zeta = \tau_1 \cup \tau_2$ and $G_{\zeta,i}$ be the (orientation preserving) affine transformation defined in Fig. 1 such that $G_{\zeta,i}(\hat{\tau}) = \tau_i$ and $G_{\zeta,i}(\hat{\zeta}) = \zeta$, with $i = 1, 2$. We define the bubble function associated with ζ by:

$$b_\zeta^K := \begin{cases} b_{\hat{\zeta}}^{\hat{K}} \circ G_{\zeta,i}^{-1}, & \text{on } \tau_i, \quad i = 1, 2, \\ 0 & \text{on } \quad \Omega \setminus \omega_\zeta. \end{cases}$$

Let $\hat{\Pi} := \{(x, y, 0) : (x, y) \in \mathbb{R}^2\}$ and let $\hat{Q} : \mathbb{R}^d \to \hat{\Pi}$ be the orthogonal projection from $\mathbb{R}^d$ to $\hat{\Pi}$. We introduce the lifting operator $\hat{P}_{\hat{\zeta}} : \mathbb{P}_k(\hat{\zeta}) \to \mathbb{P}_k(\hat{\tau})$ given by:

$$\hat{s} \longmapsto \hat{P}_{\hat{\zeta}}(\hat{s}) = \hat{s} \circ \hat{Q}.$$

Let $\tau_i \subseteq \omega_\zeta$. We define the lifting operator $P_{\zeta,\tau_i} : \mathbb{P}_k(\zeta) \to \mathbb{P}_k(\tau_i)$ by:

$$P_{\zeta,\tau_i}(s) = \hat{P}_{\hat{\zeta}}(s \circ G_{\zeta,i}) \circ G_{\zeta,i}^{-1}.$$

Using these notations, we can define a lifting operator $P_\zeta : \mathbb{P}_k(\zeta) \to \mathbb{P}_k(\omega_\zeta)$ by:

$$s \in \mathbb{P}_k(\zeta) \longmapsto P_\zeta(s) := \begin{cases} P_{\zeta,\tau_1}(s) \ \text{in } \tau_1, \\ P_{\zeta,\tau_2}(s) \ \text{in } \tau_2, \end{cases}$$

for $\boldsymbol{s} = (s_1, s_2, s_3) \in \mathbb{P}_k(\zeta)^d$, we define $\boldsymbol{P}_\zeta^K(\boldsymbol{s})$ by:

$$\boldsymbol{P}_\zeta^K(\boldsymbol{s}) = (P_\zeta(s_1), P_\zeta(s_2), P_\zeta(s_3)).$$

The next result can be prove using scaling argument.

Theorem 2 *Let $K \in \mathscr{T}_H$ and b_τ^K and b_ζ^K be the bubbles functions corresponding to $\tau \in \mathscr{T}_h^K$ and $\zeta \in \mathscr{E}_h^K$, respectively . Then:*

$$\begin{aligned}
&\|\boldsymbol{v}_h\|_{0,\tau}^2 \preceq (b_\tau^K \boldsymbol{v}_h, \boldsymbol{v}_h)_\tau \preceq \|\boldsymbol{v}_h\|_{0,\tau}^2, \\
&\|\boldsymbol{v}_h\|_{0,\tau}^2 \preceq \|b_\tau^K \boldsymbol{v}_h\|_{0,\tau} + h_\tau |b_\tau^K \boldsymbol{v}_h|_{1,\tau} \preceq \|\boldsymbol{v}_h\|_{0,\tau}, \\
&\|\boldsymbol{v}_h\|_{0,\zeta}^2 \preceq (b_\zeta^K \boldsymbol{v}_h, \boldsymbol{v}_h)_\zeta \preceq \|\boldsymbol{v}_h\|_{0,\zeta}^2, \\
&h_\tau^{-1/2} \|b_\zeta^K \boldsymbol{v}_h\|_{0,\tau} + h_\tau^{1/2} |b_\zeta^K \boldsymbol{v}_h|_{1,\tau} \preceq \|\boldsymbol{v}_h\|_{0,\zeta},
\end{aligned}$$

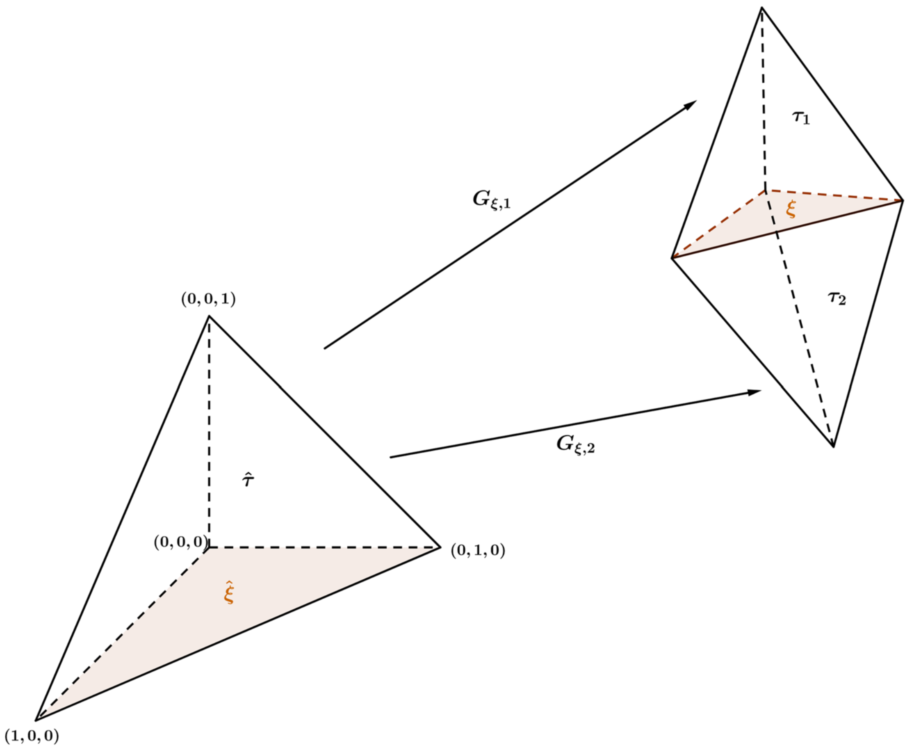

Fig. 1 Affine transformation $G_{\zeta,i}$, $i = 1, 2$ with $d = 3$

for all $\boldsymbol{v}_h \in \mathbb{P}_n(\mathscr{T}_h^K)$, $n \geq 0$.

Proof See Theorem 2.2 and Theorem 2.4 in [4]. □

Lemma 1 *We have that:*

$$\|\boldsymbol{v}\|_{0,F}^2 \preceq H_F \left\{ H_K^{-2} \|\boldsymbol{v}\|_{0,K}^2 + |\boldsymbol{v}|_{1,K}^2 \right\},$$

for all $K \in \mathscr{T}_H$, $F \subset \partial K$ *and* $\boldsymbol{v} \in \mathbf{V}(K)$.

Proof See Theorem 3.10 in [2] or (10.3.8) in [19]. □

Theorem 3 *For all* $q \in Q(K)$, *we have that:*

$$\sup_{\boldsymbol{v} \in \mathbf{V}(K)} \frac{b_K(\boldsymbol{v}, q)}{\|\boldsymbol{v}\|_{\mathbf{V}(K)}} \succeq \|q\|_{Q(K)}.$$

Proof See Theorem 2.1 in [11]. □

For each $K \in \mathscr{T}_H$, we denote by $\mathscr{C}_h^K : \mathbf{V}(K) \to \mathbf{V}_1^K$, the Clément interpolation operator, where:

$$\mathbf{V}_1^K := \left\{ \boldsymbol{v}_h \in C(K)^d : \boldsymbol{v}_h \in \mathbb{P}_1(\tau)^d, \ \forall\, \tau \in \mathscr{T}_h^K \right\}.$$

For all $\tau \in \mathscr{T}_h^K$ and all $\zeta \in \mathscr{E}_h^K$, this operator satisfies the following estimates (see [23], [29]):

$$\begin{aligned} \|\mathscr{C}_h^K(\boldsymbol{v})\|_{0,\tau} &\preceq \|\boldsymbol{v}\|_{0,\tilde{\omega}_\tau}, \\ \|\boldsymbol{v} - \mathscr{C}_h^K(\boldsymbol{v})\|_{0,\tau} &\preceq h_\tau |\boldsymbol{v}|_{1,\tilde{\omega}_\tau}, \\ \|\boldsymbol{v} - \mathscr{C}_h^K(\boldsymbol{v})\|_{0,\zeta} &\preceq h_\zeta^{1/2} |\boldsymbol{v}|_{1,\tilde{\omega}_\zeta}, \end{aligned} \tag{12}$$

for all $\boldsymbol{v} \in \mathbf{V}(K)$.

3 The MHM method

In this section, we present the MHM method as a consequence of a characterisation of the exact solution in terms of a local–global system equivalent to (8).

3.1 Characterizing the exact solution

The goal of the Multiscale Hybrid-Mixed approach is to take advantage of the local nature of problem (8), by decomposing it into independent local problems coupled with a face-based global problem. Using these ideas, the hybrid formulation (8) is equivalently to: *Find* $(\boldsymbol{u}, p, \boldsymbol{\lambda}, \rho) \in \mathbf{V} \times Q \times \boldsymbol{\Lambda} \times \mathbb{R}$ *such that:*

$$\begin{cases} (\boldsymbol{\mu}, \boldsymbol{u})_{\partial \mathscr{T}_H} = \langle \boldsymbol{\mu}, \boldsymbol{g} \rangle_{\partial\Omega} \quad \text{for all } \boldsymbol{\mu} \in \boldsymbol{\Lambda}, \\ (\xi, p)_\Omega = 0 \quad \text{for all } \xi \in \mathbb{R}, \end{cases} \tag{13}$$

$$\begin{cases} a(\boldsymbol{u}, \boldsymbol{v}) + b(\boldsymbol{v}, p) + (\boldsymbol{\lambda}, \boldsymbol{v})_{\partial \mathscr{T}_H} = (\boldsymbol{f}, \boldsymbol{v})_{\mathscr{T}_H} \quad \text{for all } \boldsymbol{v} \in \mathbf{V}, \\ b(\boldsymbol{u}, q) + (\rho, q)_\Omega = 0 \quad \text{for all } q \in Q\,. \end{cases} \tag{14}$$

Note that, due to the element-wise definition of $\mathbf{V}$, system (14) can be localised in each $K \in \mathscr{T}_H$ by testing (13)–(14) with $(\boldsymbol{v}, q, \boldsymbol{\mu}, \xi) = (\boldsymbol{v}\,|_K, q\,|_K, \mathbf{0}, 0)$. This gives us:

$$\begin{cases} a_K(\boldsymbol{u}, \boldsymbol{v}) + b_K(\boldsymbol{v}, p) = -\langle \boldsymbol{\lambda}, \boldsymbol{v} \rangle_{\partial K} + (\boldsymbol{f}, \boldsymbol{v})_K \quad \text{for all } \boldsymbol{v} \in \mathbf{V}(K), \\ b_K(\boldsymbol{u}, q) = -(\rho, q)_K \quad \text{for all } q \in Q(K). \end{cases} \tag{15}$$

Also from (15), $(\boldsymbol{u}, p)$ can be computed in terms of $\boldsymbol{\lambda}$ and ρ . Specifically, owing to the linearity of problem (15), the exact solution decomposes as follows:

$$\boldsymbol{u} = T^u \boldsymbol{\lambda} + \hat{T}^u \boldsymbol{f} + \bar{T}^u \rho \quad \text{and} \quad p = T^p \boldsymbol{\lambda} + \hat{T}^p \boldsymbol{f} + \bar{T}^p \rho, \tag{16}$$

where the functions used in (16) are given by:

- $(T^u \boldsymbol{\mu}, T^p \boldsymbol{\mu}) \in \mathbf{V} \times Q$ such that $T^u \boldsymbol{\mu}\,|_K$ and $T^p \boldsymbol{\mu}\,|_K$ satisfy:

$$\begin{cases} a_K(T^u \boldsymbol{\mu}, \boldsymbol{w}) + b_K(\boldsymbol{w}, T^p \boldsymbol{\mu}) = -\langle \boldsymbol{\mu}, \boldsymbol{w} \rangle_{\partial K} \quad \text{for all } \boldsymbol{w} \in \mathbf{V}(K), \\ b_K(T^u \boldsymbol{\mu}, q) = 0 \quad \text{for all } q \in Q(K); \end{cases} \tag{17}$$

- $(\hat{T}^u \boldsymbol{r}, \hat{T}^p \boldsymbol{r}) \in \mathbf{V} \times Q$ such that $\hat{T}^u \boldsymbol{r}\,|_K$ and $\hat{T}^p \boldsymbol{r}\,|_K$ satisfy:

$$\begin{cases} a_K(\hat{T}^u \boldsymbol{r}, \boldsymbol{w}) + b_K(\boldsymbol{w}, \hat{T}^p \boldsymbol{r}) = (\boldsymbol{f}, \boldsymbol{w})_K \quad \text{for all } \boldsymbol{w} \in \mathbf{V}(K), \\ b_K(\hat{T}^u \boldsymbol{r}, q) = 0 \quad \text{for all } q \in Q(K); \end{cases} \tag{18}$$

- $(\bar{T}^u \xi, \bar{T}^p \xi) \in \mathbf{V} \times Q$ such that $\bar{T}^u \xi\,|_K$ and $\bar{T}^p \xi\,|_K$ satisfy:

$$\begin{cases} a_K(\bar{T}^u \xi, \boldsymbol{w}) + b_K(\boldsymbol{w}, \bar{T}^p \xi) = 0 \quad \text{for all } \boldsymbol{w} \in \mathbf{V}(K), \\ b_K(\bar{T}^u \xi, q) = -(\xi, q)_K \quad \text{for all } q \in Q(K). \end{cases} \tag{19}$$

Next, testing (13) with $(\boldsymbol{v}, q, \boldsymbol{\mu}, \xi) = (\mathbf{0}, 0, \boldsymbol{\mu}, \xi)$ and using (16), we obtain the following global problem: *Find* $(\boldsymbol{\lambda}, \rho) \in \boldsymbol{\Lambda} \times \mathbb{R}$ *such that:*

$$\begin{cases} (\boldsymbol{\mu}, T^u \boldsymbol{\lambda} + \bar{T}^u \rho)_{\partial \mathscr{T}_H} = (\boldsymbol{\mu}, \boldsymbol{g})_{\partial\Omega} - (\boldsymbol{\mu}, \hat{T}^u \boldsymbol{f})_{\partial \mathscr{T}_H}, \quad \forall \boldsymbol{\mu} \in \boldsymbol{\Lambda} \\ (\xi, T^p \boldsymbol{\lambda} + \bar{T}^p \rho)_\Omega = -(\xi, \hat{T}^p \boldsymbol{f})_\Omega, \quad \forall \xi \in \mathbb{R}, \end{cases} \tag{20}$$

for all $\boldsymbol{\mu} \in \boldsymbol{\Lambda}$ and $\xi \in \mathbb{R}$.

Remark 3 Following [9], it is possible to prove that $\rho = 0$, and therefore (16) reduces to:

$$\boldsymbol{u} = T^u \boldsymbol{\lambda} + \hat{T}^u \boldsymbol{f} \quad \text{and} \quad p = T^p \boldsymbol{\lambda} + \hat{T}^p \boldsymbol{f}. \tag{21}$$

We define a local bilinear form B_K given by:

$$B_K((\boldsymbol{w}, r), (\boldsymbol{v}, q)) := a_K(\boldsymbol{w}, \boldsymbol{v}) + b_K(\boldsymbol{v}, r) - b_K(\boldsymbol{w}, q), \tag{22}$$

with $(\boldsymbol{w}, r), (\boldsymbol{v}, q) \in \mathbf{V}(K) \times Q(K)$, and naturally we denote:

$$B((\boldsymbol{w}, r), (\boldsymbol{v}, q)) := \sum_{K \in \mathscr{T}_H} B_K((\boldsymbol{w}, r), (\boldsymbol{v}, q)).$$

Theorem 4 *We have that local problems* (17)–(19) *are well–posed, and it holds:*

$$\|(\boldsymbol{w}, r)\|_{\mathbf{V}(K)\times Q(K)} \preceq \sup_{(\boldsymbol{v},q)\in \mathbf{V}(K)\times Q(K)} \frac{B_K((\boldsymbol{w}, r), (\boldsymbol{v}, q))}{\|(\boldsymbol{v}, q)\|_{\mathbf{V}(K)\times Q(K)}}.$$

Proof Thanks to Theorem 3 we have an inf–sup condition for $b_K(\cdot, \cdot)$, and using the ellipticity of $a_K(\cdot, \cdot)$, give in (7), the result follows. □

Remark 4 From (7) the coercivity of $a_K(\cdot, \cdot)$ over $\mathbf{V}(K)$ holds. Then, using Theorem 3, and the inf–sup condition, the well-posedness of (17)–(20) follows. Next, using Theorem 4 and the Riesz Representation Theorem, the bilinear form B satisfies a global inf–sup condition with a constant independent of H and h, and only depending on d_Ω, and d, respectively.

3.2 The method

The characterisation of the exact solution $(\boldsymbol{u}, p)$ in terms of the global–local system (17)–(20) yield the MHM method. Consider a finite dimensional space $\boldsymbol{\Lambda}_H$ of $\boldsymbol{\Lambda}$ such that:

$$\mathbf{\Lambda}_0 \subseteq \mathbf{\Lambda}_H \subset \mathbf{\Lambda} \cap L^2(\mathscr{E}_H)^d,$$

with:

$$\mathbf{\Lambda}_0 := \left\{ \boldsymbol{\sigma}\, \boldsymbol{n}^K\,|_F \in \mathbb{P}_0(F)^d \text{ for all } F \subset \partial K,\ K \in \mathscr{T}_H \,:\, \boldsymbol{\sigma} \in H(\mathrm{div};\Omega) \right\},$$

where $\mathbb{P}_0(F)$ is the space of constant polynomials defined on F. In this work, we search for approximating Lagrange multipliers in the space spanned by piecewise polynomial functions, i.e.:

$$\mathbf{\Lambda}_H = \mathbf{\Lambda}_l := \left\{ \boldsymbol{\mu} \in \mathbf{\Lambda} \,:\, \boldsymbol{\mu}|_{\tilde{F}} \in \mathbb{P}_l(\tilde{F})^d,\ \tilde{F} \in \mathscr{T}_{\tilde{H}}(F),\ \text{ for all } F \subset \partial K, K \in \mathscr{T}_H \right\},$$

where $\mathbb{P}_l(F)$ is the space of piecewise polynomial functions on F of degree less than or equal $l \geq 0$.

Unlike the usual interpolation choice [51], the functions in $\mathbf{\Lambda}_H$ may be discontinuous on faces $F \in \mathscr{E}_H$. Such a choice preserves the conformity of the MHM method and turns out to be central to maintaining the quality of the approximation when coefficients jump across faces. This will be explored in the numerical section.

Specifically, the solution of (20) is approximated by $(\boldsymbol{\lambda}_H, \rho_H) \in \mathbf{\Lambda}_H \times \mathbb{R}$, which is the solution to the *one-level MHM method:*

$$\begin{cases} (\boldsymbol{\mu}_H, T^u\boldsymbol{\lambda}_H + \bar{T}^u\rho_H)_{\partial\mathscr{T}_H} = (\boldsymbol{\mu}_H, \boldsymbol{g})_{\partial\Omega} - (\boldsymbol{\mu}_H, \hat{T}^u\boldsymbol{f})_{\partial\mathscr{T}_H}, \\ \quad (\xi_H, T^p\boldsymbol{\lambda}_H + \bar{T}^p\rho_H)_\Omega = -(\xi_H, \hat{T}^p\boldsymbol{f})_\Omega, \end{cases} \tag{23}$$

for all $\boldsymbol{\mu}_H \in \mathbf{\Lambda}_H$ and $\xi_H \in \mathbb{R}$, where $T^u\boldsymbol{\lambda}_H$, $\hat{T}^u\boldsymbol{f}$, $\bar{T}^u\rho_H$ and pressures $T^p\boldsymbol{\lambda}_H$, $\hat{T}^p\boldsymbol{f}$, $\bar{T}^p\rho_H$ solve (17)–(19). Thus, the *one-level* solution $(\bar{\boldsymbol{u}}_H, \bar{p}_H)$ is given through the expressions:

$$\bar{\boldsymbol{u}}_H := T^u\boldsymbol{\lambda}_H + \hat{T}^u\boldsymbol{f} + \bar{T}^u\rho_H \quad \text{and} \quad \bar{p}_H := T^p\boldsymbol{\lambda}_H + \hat{T}^p\boldsymbol{f} + \bar{T}^p\rho_H.$$

Note that to make the one-level MHM method effective, we need to solve local problems (17)–(19), exactly, which is, en general, not possible. To overcome this, we introduce the *two-level MHM method* which consists of: *Find* $(\boldsymbol{\lambda}_{H,h}, \rho_H) \in \mathbf{\Lambda}_H \times \mathbb{R}$ *such that:*

$$\begin{cases} (\boldsymbol{\mu}_H, T_h^u\boldsymbol{\lambda}_{H,h} + \bar{T}_h^u\rho_H)_{\partial\mathscr{T}_H} = (\boldsymbol{\mu}_H, \boldsymbol{g})_{\partial\Omega} - (\boldsymbol{\mu}_H, \hat{T}_h^u\boldsymbol{f})_{\partial\mathscr{T}_H}, \\ \quad (\xi_H, T_h^p\boldsymbol{\lambda}_{H,h} + \bar{T}_h^p\rho_H)_\Omega = -(\xi_H, \hat{T}_h^p\boldsymbol{f})_\Omega, \end{cases} \tag{24}$$

for all $(\boldsymbol{\mu}_H, \xi_H) \in \mathbf{\Lambda}_H \times \mathbb{R}$. In this work, we adopt a stabilised finite element method [15] to approximate the solution of the local problems (17)–(19) computing the approximated velocities $T_h^u\boldsymbol{\lambda}_{H,h}$, $\hat{T}_h^u\boldsymbol{f}$, $\bar{T}_h^u\rho_H$ and pressures $T_h^p\boldsymbol{\lambda}_{H,h}$, $\hat{T}_h^p\boldsymbol{f}$, $\bar{T}_h^p\rho_H$.

As such, the two-level discrete solution $(\boldsymbol{u}_{H,h}, p_{H,h})$ is given through the expressions:

$$\boldsymbol{u}_{H,h} := T_h^u\boldsymbol{\lambda}_{H,h} + \hat{T}_h^u\boldsymbol{f} + \bar{T}_h^u\rho_H \quad \text{and} \quad p_{H,h} := T_h^p\boldsymbol{\lambda}_{H,h} + \hat{T}_h^p\boldsymbol{f} + \bar{T}_h^p\rho_H.$$

Such a choice makes the appealing option of using equal-order nodal pairs of interpolation spaces for the velocity and the pressure variables (i.e. $k = n$ in (10) and (11)) as the second-level solver. For completeness, we recall (see [15] for details) that this scheme consists of: *Find* $(\boldsymbol{u}, p) \in \mathbf{V}_h(K) \times Q_h(K)$ *such that:*

$$B_K^s((\boldsymbol{u}, p), (\boldsymbol{v}, q)) = F_K^s(\boldsymbol{v}, q) \quad \text{for all } (\boldsymbol{v}, q) \in \mathbf{V}_h(K) \times Q_h(K), \tag{25}$$

where:

$$B_K^s((\boldsymbol{u},p),(\boldsymbol{v},q)) := B_K((\boldsymbol{u},p),(\boldsymbol{v},q)) + \sum_{\tau\in\mathscr{T}_h^K} \kappa_\tau(\nabla\cdot\boldsymbol{u},\nabla\cdot\boldsymbol{v})_\tau \\ - \sum_{\tau\in\mathscr{T}_h^K} \delta_\tau(-\nu\Delta\boldsymbol{u} + (\nabla\boldsymbol{u})\boldsymbol{\alpha} + \gamma\,\boldsymbol{u} + \nabla p, -\nu\Delta\boldsymbol{v} - (\nabla\boldsymbol{v})\boldsymbol{\alpha} + \gamma\,\boldsymbol{v} - \nabla q)_\tau,$$

and

$$F_K^s(\boldsymbol{v},q) := F_K(\boldsymbol{v},q) - \sum_{\tau\in\mathscr{T}_h^K} \delta_\tau(\boldsymbol{f}, -\nu\Delta\boldsymbol{v} - (\nabla\boldsymbol{v})\boldsymbol{\alpha} + \gamma\,\boldsymbol{v} - \nabla q)_\tau.$$

The stabilisation parameters are given by:

$$\kappa_\tau := \|\boldsymbol{\alpha}\|_{\infty,\tau}\, h_\tau\, \min\{1, Pe_\tau^A\}, \text{ and } \delta_\tau := \frac{h_\tau^2}{\gamma h_\tau^2 \max\left\{1, Pe_\tau^R\right\} + \frac{4\,\nu}{m_\tau} \max\left\{1, Pe_\tau^A\right\}}, \tag{26}$$

where the local *Péclet* numbers are defined by:

$$Pe_\tau^R := \frac{4\,\nu}{\gamma\, h_\tau^2\, m_\tau} \qquad \text{and} \qquad Pe_\tau^A := \frac{m_\tau \|\boldsymbol{\alpha}\|_{\infty,\tau} h_\tau}{4\nu}.$$

and $m_\tau := \min\left\{\frac{1}{3}, C_k\right\}$ with:

$$C_k\, h_\tau^2\, \|\Delta\boldsymbol{v}\|_{0,\tau}^2 \leq \|\nabla\boldsymbol{v}\|_{0,\tau}^2 \quad \text{for all } \boldsymbol{v}\in\mathbf{V}_h(K). \tag{27}$$

Here C_k is a constant that depends only on d and the polynomial degree chosen for the velocity (see [35]).

Owing to definitions (25)–(27), the local solutions in (17)–(19) are approximated, in each $K\in\mathscr{T}_H$, by the solutions of the following discrete problems:

– *Find* $(T_h^u\boldsymbol{\lambda}_{H,h}, T_h^p\boldsymbol{\lambda}_{H,h})\in\mathbf{V}_h(K)\times Q_h(K)$ *such that:*

$$B_K^s((T_h^u\boldsymbol{\lambda}_{H,h}, T_h^p\boldsymbol{\lambda}_{H,h}),(\boldsymbol{v},q)) = -\langle\boldsymbol{\lambda}_{H,h},\boldsymbol{v}\rangle_{\partial K} \text{ for all } (\boldsymbol{v},q)\in\mathbf{V}_h(K)\times Q_h(K); \tag{28}$$

– *Find* $(\hat{T}_h^u\boldsymbol{f}, \hat{T}_h^p\boldsymbol{f})\in\mathbf{V}_h(K)\times Q_h(K)$ *such that:*

$$B_K^s((\hat{T}_h^u\boldsymbol{f}, \hat{T}_h^p\boldsymbol{f}),(\boldsymbol{v},q)) = F_K^s(\boldsymbol{v},q) \text{ for all } (\boldsymbol{v},q)\in\mathbf{V}_h(K)\times Q_h(K); \tag{29}$$

– *Find* $(\bar{T}_h^u\rho_H, \bar{T}_h^p\rho_H)\in\mathbf{V}_h(K)\times Q_h(K)$ *such that:*

$$B_K^s((\bar{T}_h^u\rho_H, \bar{T}_h^p\rho_H),(\boldsymbol{v},q)) = (\rho_H,q)_K \text{ for all } (\boldsymbol{v},q)\in\mathbf{V}_h(K)\times Q_h(K). \tag{30}$$

Remark 5 As in the continuous case, in the discrete case, we can prove that $\rho_H = 0$, following the same ideas from [9] and hence the solutions of the one-level and two-level MHM methods, can be characterised as follows:

$$\bar{\boldsymbol{u}}_H := T^u\boldsymbol{\lambda}_H + \hat{T}^u\boldsymbol{f} \quad \text{and} \quad \bar{p}_H := T^p\boldsymbol{\lambda}_H + \hat{T}^p\boldsymbol{f}, \tag{31}$$

$$\boldsymbol{u}_{H,h} := T_h^u\boldsymbol{\lambda}_{H,h} + \hat{T}_h^u\boldsymbol{f} \quad \text{and} \quad p_{H,h} := T_h^p\boldsymbol{\lambda}_{H,h} + \hat{T}_h^p\boldsymbol{f}. \tag{32}$$

4 A multiscale a posteriori error estimator

In this section, we define a two-level residual error estimator. Let η_1 be the *first-level a posteriori error estimator*, given by:

$$\eta_1 := \left\{ \sum_{K\in\mathscr{T}_H} \sum_{F\subset\partial K} \eta_{1,F}^2 \right\}^{1/2},$$

where:

$$\eta_{1,F} := \frac{\|\boldsymbol{R}_F\|_{0,F}}{H_F^{1/2}},$$

with:

$$\boldsymbol{R}_F := \begin{cases} -\frac{1}{2}\,[\![\boldsymbol{u}_{H,h}]\!]\,, & F\in\mathscr{E}_0, \\ \boldsymbol{g}-\boldsymbol{u}_{H,h}, & F\in\mathscr{E}_H\setminus\mathscr{E}_0. \end{cases}$$

Recalling that, $\{\mathscr{T}_h^K\}_{h>0}$ is a regular family of triangulations of $K\in\mathscr{T}_H$, we define residuals over each $\tau\in\mathscr{T}_h^K$ and $\zeta\in\mathscr{E}_h^K$, respectively, as follows:

$$\boldsymbol{R}_\tau^K := \big(\nu\Delta\boldsymbol{u}_{H,h} - (\nabla\boldsymbol{u}_{H,h})\boldsymbol{\alpha} - \gamma\boldsymbol{u}_{H,h} - \nabla p_{H,h} + \boldsymbol{f}\big)|_\tau,$$

and

$$\boldsymbol{R}_\zeta^K := \begin{cases} \left[\!\!\left[-\nu\dfrac{\partial\boldsymbol{u}_{H,h}}{\partial\boldsymbol{n}_\zeta^\tau} + p_{H,h}\boldsymbol{n}_\zeta^\tau + \dfrac{1}{2}(\boldsymbol{u}_{H,h}\otimes\boldsymbol{\alpha})\boldsymbol{n}_\zeta^\tau \right]\!\!\right] & \text{on } \zeta\in\mathscr{E}_0^K, \\ -\boldsymbol{\lambda}_{H,h} - \nu\dfrac{\partial\boldsymbol{u}_{H,h}}{\partial\boldsymbol{n}_\zeta^\tau} + p_{H,h}\boldsymbol{n}_\zeta^\tau + \dfrac{1}{2}(\boldsymbol{u}_{H,h}\otimes\boldsymbol{\alpha})\boldsymbol{n}_\zeta^\tau & \text{on } \zeta\in\mathscr{E}_b^K. \end{cases}$$

Its global version reads:

$$\eta_{2,K} := \left\{ \sum_{\tau\in\mathscr{T}_h^K} \left(h_\tau^2\|\boldsymbol{R}_\tau^K\|_{0,\tau}^2 + \|\nabla\cdot\boldsymbol{u}_{H,h}\|_{0,\tau}^2 \right) + \sum_{\zeta\in\mathscr{E}_h^K} h_\zeta\|\boldsymbol{R}_\zeta^K\|_{0,\zeta}^2 \right\}^{1/2}, \qquad (33)$$

and, thus, the *global second-level estimator* is defined by:

$$\eta_2 := \frac{1}{2^{2l}}\left[\sum_{K\in\mathscr{T}_H}\eta_{2,K}^2\right]^{1/2},$$

where l is the polynomial degree on faces. Summing up first- and second-level contributions, the global a posteriori error estimator η reads:

$$\eta := \eta_1 + \eta_2. \qquad (34)$$

Remark 6 Note that the definition of η_1 is inspired by the a posteriori error estimator proposed in [11] for the Stokes and Brinkman equation and in [39] for the reaction–diffusion–advection problem in the first-level mesh. The second-level error estimator η_2 was introduced in [6] for the Stokes equations (also see the estimator in the second-level mesh in [11]).

4.1 Technical results

In this subsection, we introduce some technical results that will be useful to establish our main results. First, we present a residual functional which can be characterised in terms of local residuals on each $\tau \in \mathscr{T}_h^K$ and $\zeta \in \mathscr{E}_h^K$.

Lemma 2 *Let $(\boldsymbol{u}_{H,h}, p_{H,h})$ be the solution of two-level MHM method given by (32). Define the local residual functional $\boldsymbol{R}_h^K : \mathbf{V}(K) \to \mathbb{R}$, by:*

$$\boldsymbol{R}_h^K(\boldsymbol{v}) := (\boldsymbol{f}, \boldsymbol{v})_K - \langle \boldsymbol{\lambda}_{H,h}, \boldsymbol{v}\rangle_{\partial K} - a_K(\boldsymbol{u}_{H,h}, \boldsymbol{v}) - b_K(p_{H,h}, \boldsymbol{v}),$$

for all $\boldsymbol{v} \in \mathbf{V}(K)$. Then:

$$\boldsymbol{R}_h^K(\boldsymbol{v}) = \sum_{\tau \in \mathscr{T}_h^K} (\boldsymbol{R}_\tau^K, \boldsymbol{v})_\tau + \sum_{\zeta \in \mathscr{E}_h^K} (\boldsymbol{R}_\zeta^K, \boldsymbol{v})_\zeta,$$

for all $\boldsymbol{v} \in \mathbf{V}(K)$.

Proof Using the identity (4) on each $\tau \in \mathscr{T}_h^K$, equations (17) and (18), and integrating by parts, we have that:

$$\begin{aligned}
\boldsymbol{R}_h^K(\boldsymbol{v}) &= -\langle \boldsymbol{\lambda}_{H,h}, \boldsymbol{v}\rangle_{\partial K} + (\boldsymbol{f}, \boldsymbol{v})_K - \nu\,(\nabla \boldsymbol{u}_{H,h}, \boldsymbol{v})_K - \frac{1}{2}((\nabla \boldsymbol{u}_{H,h})\boldsymbol{\alpha}, \boldsymbol{v})_K \\
&\quad + \frac{1}{2}(\boldsymbol{u}_{H,h}, (\nabla \boldsymbol{v})\boldsymbol{\alpha})_K - (\gamma_0 \boldsymbol{u}_{H,h}, \boldsymbol{v})_K + (\nabla\cdot\boldsymbol{v}, p_{H,h})_K \\
&= -\langle \boldsymbol{\lambda}_{H,h}, \boldsymbol{v}\rangle_{\partial K} + \sum_{\tau \in \mathscr{T}_h^K} \Big[(\boldsymbol{f}, \boldsymbol{v})_\tau - \nu\,(\nabla \boldsymbol{u}_{H,h}, \boldsymbol{v})_\tau - \frac{1}{2}((\nabla \boldsymbol{u}_{H,h})\boldsymbol{\alpha}, \boldsymbol{v})_\tau \\
&\quad + \frac{1}{2}(\boldsymbol{u}_{H,h}, (\nabla \boldsymbol{v})\boldsymbol{\alpha})_\tau - (\gamma_0 \boldsymbol{u}_{H,h}, \boldsymbol{v}) + (\nabla\cdot\boldsymbol{v}, p_{H,h})_\tau \Big] \\
&= -\langle \boldsymbol{\lambda}_{H,h}, \boldsymbol{v}\rangle_{\partial K} + \sum_{\tau \in \mathscr{T}_h^K} \Big[(\boldsymbol{f}, \boldsymbol{v})_\tau + \nu\,(\Delta \boldsymbol{u}_{H,h}, \boldsymbol{v})_\tau \\
&\quad - \left(\frac{\partial \boldsymbol{u}_{H,h}}{\partial \boldsymbol{n}^\tau}, \boldsymbol{v}\right)_{\partial\tau} - ((\nabla \boldsymbol{u}_{H,h})\boldsymbol{\alpha}, \boldsymbol{v})_\tau - \frac{1}{2}((\nabla\cdot\boldsymbol{\alpha})\boldsymbol{u}_{H,h}, \boldsymbol{v})_\tau + \frac{1}{2}((\boldsymbol{\alpha}\cdot\boldsymbol{n}^\tau)\boldsymbol{u}_{H,h}, \boldsymbol{v})_{\partial\tau} \\
&\quad - \left(\left(\gamma - \frac{1}{2}(\nabla\cdot\boldsymbol{\alpha})\right)\boldsymbol{u}_{H,h}, \boldsymbol{v}\right)_\tau - (\nabla p_{H,h}, \boldsymbol{v})_\tau + (p_{H,h}\boldsymbol{n}^\tau, \boldsymbol{v})_{\partial\tau} \Big] \\
&= \sum_{\zeta \in \mathscr{E}_0^K} \left(\left[\!\!\left[-\nu \frac{\partial \boldsymbol{u}_{H,h}}{\partial \boldsymbol{n}_\zeta^\tau} + p_{H,h}\boldsymbol{n}_\zeta^\tau + \frac{1}{2}(\boldsymbol{\alpha}\cdot\boldsymbol{n}_\zeta^\tau)\boldsymbol{u}_{H,h} \right]\!\!\right], \boldsymbol{v} \right) \\
&\quad + \sum_{\zeta \in \mathscr{E}_b^K} \left(-\boldsymbol{\lambda}_{H,h} - \nu \frac{\partial \boldsymbol{u}_{H,h}}{\partial \boldsymbol{n}_\zeta^\tau} + p_{H,h}\boldsymbol{n}_\zeta^\tau + \frac{1}{2}(\boldsymbol{\alpha}\cdot\boldsymbol{n}_\zeta^\tau)\boldsymbol{u}_{H,h}, \boldsymbol{v} \right) + \sum_{\tau \in \mathscr{T}_h^K} (\boldsymbol{R}_\tau^K, \boldsymbol{v})_\tau \\
&= \sum_{\tau \in \mathscr{T}_h^K} (\boldsymbol{R}_\tau^K, \boldsymbol{v})_\tau + \sum_{\zeta \in \mathscr{E}_h^K} (\boldsymbol{R}_\zeta^K, \boldsymbol{v})_\zeta,
\end{aligned}$$

which conclude the proof. □

In the sequel, we will need the following notation:

$$u_H := T^u \boldsymbol{\lambda}_{H,h} + \hat{T}^u \boldsymbol{f} \qquad \text{and} \qquad p_H := T^p \boldsymbol{\lambda}_{H,h} + \hat{T}^p \boldsymbol{f}, \tag{35}$$

and the next intermediate result.

Lemma 3 *The following estimate holds:*

$$\|(\boldsymbol{u}_H - \boldsymbol{u}_{H,h}, p_H - p_{H,h})\|_{\mathbf{V}(K)\times Q(K)} \preceq \eta_{2,K},$$

for all $K \in \mathscr{T}_H$.

Proof Let us define $(\boldsymbol{e}^{\boldsymbol{u}}, e^p) := (\boldsymbol{u}_H - \boldsymbol{u}_{H,h}, p_H - p_{H,h})$. From (17), (18), (22), and Lemma 2, we have:

$$\begin{aligned} B_K((\boldsymbol{e}^{\boldsymbol{u}}, e^p), (\boldsymbol{v}, q)) &= B_K((\boldsymbol{u}_H, p_H), (\boldsymbol{v}, q)) - B_K((\boldsymbol{u}_{H,h}, p_{H,h}), (\boldsymbol{v}, q)) \\ &= -\langle \boldsymbol{\lambda}_{H,h}, \boldsymbol{v}\rangle_{\partial K} + (\boldsymbol{f}, \boldsymbol{v})_K - B_K((\boldsymbol{u}_{H,h}, p_{H,h}), (\boldsymbol{v}, q)) \\ &= \boldsymbol{R}_h^K(\boldsymbol{v}) + b_K(\boldsymbol{u}_{H,h}, q) \\ &= \sum_{\tau\in\mathscr{T}_h^K} \left[(\boldsymbol{R}_\tau^K, \boldsymbol{v})_\tau + (\nabla\cdot \boldsymbol{u}_{H,h}, q)_\tau\right] + \sum_{\zeta\in\mathscr{E}_h^K} (\boldsymbol{R}_\zeta^K, \boldsymbol{v})_\zeta, \end{aligned} \tag{36}$$

for all $\boldsymbol{v} \in \mathbf{V}(K)$ and $q \in Q(K)$. For $K \in \mathscr{T}_H$, let $\boldsymbol{v}_h := \mathscr{C}_h^K(\boldsymbol{v})$ with $\boldsymbol{v} \in \mathbf{V}(K)$. Then, replacing $\boldsymbol{v}$ by $\boldsymbol{v} - \boldsymbol{v}_h$ in (36) and using Cauchy–Schwarz inequality, we get:

$$\begin{aligned} &B_K((\boldsymbol{e}^{\boldsymbol{u}}, e^p), (\boldsymbol{v} - \boldsymbol{v}_h, q)) \\ &\quad\le \sum_{\tau\in\mathscr{T}_h^K} \left[\|\boldsymbol{R}_\tau^K\|_{0,\tau}\|\boldsymbol{v} - \boldsymbol{v}_h\|_{0,\tau} + \|\nabla\cdot\boldsymbol{u}_{H,h}\|_{0,\tau}\|q\|_{0,\tau}\right] \\ &\quad + \sum_{\zeta\in\mathscr{E}_h^K} \|\boldsymbol{R}_\zeta^K\|_{0,\zeta}\|\boldsymbol{v} - \boldsymbol{v}_h\|_{0,\zeta}. \end{aligned} \tag{37}$$

On other hand, using (22), (28), and (29), and taking $(\boldsymbol{v}, q) = (\boldsymbol{v}_h, 0)$, we get:

$$\begin{aligned} &B_K((\boldsymbol{e}^{\boldsymbol{u}}, e^p), (\boldsymbol{v}_h, 0)) \\ &= a_K(\boldsymbol{u}_H - \boldsymbol{u}_{H,h}, \boldsymbol{v}_h) + b_K(\boldsymbol{v}_h, p_H - p_{H,h}) \\ &= a_K(\boldsymbol{u}_H, \boldsymbol{v}_h) + b_K(\boldsymbol{v}_h, p_H) - \left[a_K(\boldsymbol{u}_{H,h}, \boldsymbol{v}_h) + b_K(\boldsymbol{v}_h, p_{H,h})\right] \\ &= -\langle \boldsymbol{\lambda}_{H,h}, \boldsymbol{v}_h\rangle_{\partial K} + (\boldsymbol{f}, \boldsymbol{v}_h)_K - \Big[a_K(T_h^u \boldsymbol{\lambda}_{H,h}, \boldsymbol{v}_h) + b_K(\boldsymbol{v}_h, T_h^p \boldsymbol{\lambda}_{H,h}) \\ &\quad + a_K(\hat{T}_h^u \boldsymbol{f}, \boldsymbol{v}_h) + b_K(\boldsymbol{v}_h, \hat{T}_h^p \boldsymbol{f})\Big] \\ &= \sum_{\tau\in\mathscr{T}_h^K} \delta_\tau(\nu\Delta\boldsymbol{u}_{H,h} - (\nabla\boldsymbol{u}_{H,h})\boldsymbol{\alpha} - \gamma\boldsymbol{u}_{H,h} - \nabla p_{H,h} + \boldsymbol{f}, -\nu\Delta\boldsymbol{v}_h - (\nabla\boldsymbol{v}_h)\boldsymbol{\alpha} + \gamma\boldsymbol{v}_h)_\tau \\ &\quad + \sum_{\tau\in\mathscr{T}_h^K} \kappa_\tau(\nabla\cdot\boldsymbol{u}_{H,h}, \nabla\cdot\boldsymbol{v}_h)_\tau \\ &= \sum_{\tau\in\mathscr{T}_h^K} \left[\delta_\tau(\boldsymbol{R}_\tau^K, -\nu\Delta\boldsymbol{v}_h - (\nabla\boldsymbol{v}_h)\boldsymbol{\alpha} + \gamma\boldsymbol{v}_h)_\tau + \kappa_\tau(\nabla\cdot\boldsymbol{u}_{H,h}, \nabla\cdot\boldsymbol{v}_h)_\tau\right]. \end{aligned} \tag{38}$$

From the definition of δ_τ in (26), it is possible to show that $\delta_\tau \leq \min\left\{\dfrac{h_\tau^2}{12\nu}, \dfrac{h_\tau}{\|\boldsymbol{\alpha}\|_\infty}\right\}$, thus using (27), we get:

$$\begin{aligned}
&\delta_\tau \| -\nu\Delta \boldsymbol{v}_h - (\nabla \boldsymbol{v}_h)\boldsymbol{\alpha} + \gamma \boldsymbol{v}_h\|_{0,\tau} \\
&\leq \nu C_k^{-1}\delta_\tau h_\tau^{-1}\|\nabla \boldsymbol{v}_h\|_{0,\tau} + \delta_\tau \|\boldsymbol{\alpha}\|_\infty \|\nabla \boldsymbol{v}_h\|_{0,\tau} + \delta_\tau \gamma \|\boldsymbol{v}_h\|_{0,\tau} \\
&\leq C_k^{-1} h_\tau \|\nabla \boldsymbol{v}_h\|_{0,\tau} + h_\tau \|\nabla \boldsymbol{v}_h\|_{0,\tau} + \frac{\gamma}{\|\boldsymbol{\alpha}\|_\infty} h_\tau \|\boldsymbol{v}_h\|_{0,\tau} \\
&\preceq h_\tau \|\boldsymbol{v}_h\|_{1,\tau}.
\end{aligned} \tag{39}$$

Now, using the fact that $\kappa_\tau \leq \|\boldsymbol{\alpha}\|_\infty h_\tau$, and an inverse inequality, we get:

$$\begin{aligned}
\kappa_\tau(\nabla\cdot \boldsymbol{u}_{H,h}, \nabla \cdot \boldsymbol{v}_h)_{0,\tau} &\leq \kappa_\tau \|\nabla \cdot \boldsymbol{u}_{H,h}\|_{0,\tau}\|\nabla\cdot \boldsymbol{v}_h\|_{0,\tau} \leq \sqrt{d}\,\|\boldsymbol{\alpha}\|_{\infty,\tau} h_\tau \|\nabla\cdot \boldsymbol{u}_{H,h}\|_{0,\tau}\|\nabla \boldsymbol{v}_h\|_{0,\tau} \\
&\preceq \|\nabla\cdot \boldsymbol{u}_{H,h}\|_{0,\tau}\|\boldsymbol{v}_h\|_{0,\tau}.
\end{aligned} \tag{40}$$

Finally, using (37)–(40), the properties (12), Cauchy-Schwarz inequality, and mesh regularity, we arrive at:

$$\begin{aligned}
&B_K\left((\boldsymbol{e}^{\boldsymbol{u}}, e^p), (\boldsymbol{v}, q)\right) \\
&\quad = B_K((\boldsymbol{e}^{\boldsymbol{u}}, e^p), (\boldsymbol{v} - \boldsymbol{v}_h, q)) + B_K((\boldsymbol{e}^{\boldsymbol{u}}, e^p), (\boldsymbol{v}_h, 0)) \\
&\quad \preceq \sum_{\tau\in\mathscr{T}_h^K}\left[\|\boldsymbol{R}_\tau^K\|_{0,\tau}\|\boldsymbol{v}-\boldsymbol{v}_h\|_{0,\tau} + \|\nabla\cdot \boldsymbol{u}_{H,h}\|_{0,\tau}\|q\|_{0,\tau}\right] + \sum_{\zeta\in\mathscr{E}_h^K}\|\boldsymbol{R}_\zeta^K\|_{0,\zeta}\|\boldsymbol{v}-\boldsymbol{v}_h\|_{0,\zeta} \\
&\qquad + \sum_{\tau\in\mathscr{T}_h^K}\|\nabla\cdot \boldsymbol{u}_{H,h}\|_{0,\tau}\|\boldsymbol{v}_h\|_{0,\tau} + \sum_{\tau\in\mathscr{T}_h^K} h_\tau\|\boldsymbol{R}_\tau^K\|_{0,\tau}\|\boldsymbol{v}_h\|_{1,\tau} \\
&\quad \preceq \sum_{\tau\in\mathscr{T}_h^K}\left[h_\tau\|\boldsymbol{R}_\tau^K\|_{0,\tau}|\boldsymbol{v}|_{1,\tilde{\omega}_\tau} + \|\nabla\cdot \boldsymbol{u}_{H,h}\|_{0,\tau}\|q\|_{0,\tau}\right] + \sum_{\zeta\in\mathscr{E}_h^K} h_\zeta^{1/2}\|\boldsymbol{R}_\zeta^K\|_{0,\zeta}|\boldsymbol{v}|_{1,\tilde{\omega}_\zeta} \\
&\qquad + \sum_{\tau\in\mathscr{T}_h^K}\|\nabla\cdot \boldsymbol{u}_{H,h}\|_{0,\tau}\|\boldsymbol{v}_h\|_{0,\tau} + \sum_{\tau\in\mathscr{T}_h^K} h_\tau\|\boldsymbol{R}_\tau^K\|_{0,\tau}\|\boldsymbol{v}_h\|_{1,\tau} \\
&\quad \preceq \left\{\sum_{\tau\in\mathscr{T}_h^K}\left[h_\tau^2\|\boldsymbol{R}_\tau^K\|_{0,\tau}^2 + \|\nabla\cdot \boldsymbol{u}_{H,h}\|_{0,\tau}^2 + \sum_{\zeta\in\mathscr{E}_h^K} h_\zeta\|\boldsymbol{R}_\zeta^K\|_{0,\zeta}^2\right]\right\}^{1/2} \times \\
&\qquad \left\{\sum_{\tau\in\mathscr{T}_h^K}\left[|\boldsymbol{v}|_{1,\tilde{\omega}_\tau}^2 + \|q\|_{0,\tau}^2 + \|\boldsymbol{v}\|_{1,\tau}^2\right] + \sum_{\zeta\in\mathscr{E}_h^K}|\boldsymbol{v}|_{1,\tilde{\omega}_\tau}^2\right\}^{1/2} \\
&\quad \preceq \eta_{2,K}\,\|(\boldsymbol{v}, q)\|_{\mathbf{V}(K)\times Q(K)}.
\end{aligned}$$

Finally, applying Theorem 4, we get the desired result. □

Remark 7 Note that testing (28) with $(\boldsymbol{v}, q) = (\mathbf{0}, 1|_K)$, we get:

$$\int_K \nabla \cdot T_h^u \boldsymbol{\lambda}_{H,h} = 0,$$

and using the analogous equation for the one-level MHM method, we can prove that:

$$\int_K \nabla \cdot T^u \boldsymbol{\lambda}_H = 0.$$

Lemma 4 *Let $\boldsymbol{\lambda} \in \boldsymbol{\Lambda}$ and $\boldsymbol{\lambda}_H \in \boldsymbol{\lambda}_{H,h}$ be the solutions of problems (20) and (24) respectively. Then, we have:*

$$\|T^p(\boldsymbol{\lambda} - \boldsymbol{\lambda}_{H,h})\|_Q \preceq \|T^u(\boldsymbol{\lambda} - \boldsymbol{\lambda}_{H,h})\|_{\mathbf{V}} + \eta_2.$$

Proof Let $\boldsymbol{w} := \frac{1}{d}\boldsymbol{x} \in H^1(\Omega)^d$, then $\nabla \cdot \boldsymbol{w} = 1$ and $\nabla \boldsymbol{w} = \frac{1}{d}\mathbf{I}$. Then, using the first equation from (17), (28), and the Remark 7, we have:

$$\begin{aligned}
\int_K T^p \boldsymbol{\lambda}_{H,h}\, dx &= a_K(T^u \boldsymbol{\lambda}_{H,h}, \boldsymbol{w}) + \langle \boldsymbol{\lambda}_{H,h}, \boldsymbol{w}\rangle_{\partial K} \\
&= \nu(\nabla T^u \boldsymbol{\lambda}_{H,h}, \nabla \boldsymbol{w})_K + \frac{1}{2}((\nabla T^u \boldsymbol{\lambda}_{H,h})\boldsymbol{\alpha}, \boldsymbol{w})_K - \frac{1}{2}(T^u \boldsymbol{\lambda}_{H,h}, (\nabla \boldsymbol{w})\boldsymbol{\alpha})_K + (\gamma_0\, T^u \boldsymbol{\lambda}_{H,h}, \boldsymbol{w})_K + \langle \boldsymbol{\lambda}_{H,h}, \boldsymbol{w}\rangle_{\partial K} \\
&= \frac{\nu}{d}\int_K \nabla \cdot T^u \boldsymbol{\lambda}_{H,h}\, dx + \frac{1}{2}((\nabla T^u \boldsymbol{\lambda}_{H,h})\boldsymbol{\alpha}, \boldsymbol{w})_K - \frac{1}{2}(T^u \boldsymbol{\lambda}_{H,h}, (\nabla \boldsymbol{w})\boldsymbol{\alpha})_K + (\gamma_0\, T^u \boldsymbol{\lambda}_{H,h}, \boldsymbol{w})_K + \langle \boldsymbol{\lambda}_{H,h}, \boldsymbol{w}\rangle_{\partial K} \\
&= \frac{\nu}{d}\int_K \nabla \cdot T_h^u \boldsymbol{\lambda}_{H,h} dx + \frac{1}{2}((\nabla T^u \boldsymbol{\lambda}_{H,h})\boldsymbol{\alpha}, \boldsymbol{w})_K - \frac{1}{2}(T^u \boldsymbol{\lambda}_{H,h}, (\nabla \boldsymbol{w})\boldsymbol{\alpha})_K + (\gamma_0\, T^u \boldsymbol{\lambda}_{H,h}, \boldsymbol{w})_K + \langle \boldsymbol{\lambda}_{H,h}, \boldsymbol{w}\rangle_{\partial K} \\
&= \nu(\nabla T_h^u \boldsymbol{\lambda}_{H,h}, \nabla \boldsymbol{w})_K + \frac{1}{2}((\nabla T^u \boldsymbol{\lambda}_{H,h})\boldsymbol{\alpha}, \boldsymbol{w})_K - \frac{1}{2}(T^u \boldsymbol{\lambda}_{H,h}, (\nabla \boldsymbol{w})\boldsymbol{\alpha})_K + (\gamma_0\, T^u \boldsymbol{\lambda}_{H,h}, \boldsymbol{w})_K + \langle \boldsymbol{\lambda}_{H,h}, \boldsymbol{w}\rangle_{\partial K} \\
&= -\frac{1}{2}((\nabla T_h^u \boldsymbol{\lambda}_{H,h})\boldsymbol{\alpha}, \boldsymbol{w})_K + \frac{1}{2}(T_h^u \boldsymbol{\lambda}_{H,h}, (\nabla \boldsymbol{w})\boldsymbol{\alpha})_K - (\gamma_0\, T_h^u \boldsymbol{\lambda}_{H,h}, \boldsymbol{w})_K + (\nabla \cdot \boldsymbol{w}, T_h^p \boldsymbol{\lambda}_{H,h})_K \\
&\quad + \sum_{\tau \in \mathcal{T}_h^K} \delta_\tau(-\nu\Delta T_h^u \boldsymbol{\lambda}_{H,h} + (\nabla T_h^u \boldsymbol{\lambda}_{H,h})\boldsymbol{\alpha} + \gamma T_h^u \boldsymbol{\lambda}_{H,h} + \nabla T_h^p \boldsymbol{\lambda}_{H,h}, -(\nabla \boldsymbol{w})\boldsymbol{\alpha} + \gamma \boldsymbol{w})_\tau \\
&\quad - \sum_{\tau \in \mathcal{T}_h^K} \kappa_\tau(\nabla \cdot T_h^u \boldsymbol{\lambda}_{H,h}, \nabla \cdot \boldsymbol{w})_\tau + \frac{1}{2}((\nabla T^u \boldsymbol{\lambda}_H)\boldsymbol{\alpha}, \boldsymbol{w})_K - \frac{1}{2}(T^u \boldsymbol{\lambda}_H, (\nabla \boldsymbol{w})\boldsymbol{\alpha})_K + (\gamma_0\, T^u \boldsymbol{\lambda}_H, \boldsymbol{w})_K \\
&= \int_K T_h^p \boldsymbol{\lambda}_{H,h} dx + \frac{1}{2}\big(\nabla(T^u \boldsymbol{\lambda}_H - T_h^u \boldsymbol{\lambda}_{H,h})\boldsymbol{\alpha}, \boldsymbol{w}\big)_K - \frac{1}{2}(T^u \boldsymbol{\lambda}_H - T_h^u \boldsymbol{\lambda}_{H,h}, (\nabla \boldsymbol{w})\boldsymbol{\alpha})_K + (\gamma_0\,(T^u \boldsymbol{\lambda}_H - T_h^u \boldsymbol{\lambda}_{H,h}), \boldsymbol{w})_K \\
&\quad + \sum_{\tau \in \mathcal{T}_h^K} \delta_\tau(-\nu\Delta T_h^u \boldsymbol{\lambda}_{H,h} + (\nabla T_h^u \boldsymbol{\lambda}_{H,h})\boldsymbol{\alpha} + \gamma T_h^u \boldsymbol{\lambda}_{H,h} + \nabla T_h^p \boldsymbol{\lambda}_{H,h}, -(\nabla \boldsymbol{w})\boldsymbol{\alpha} + \gamma \boldsymbol{w})_\tau \\
&\quad - \sum_{\tau \in \mathcal{T}_h^K} \kappa_\tau(\nabla \cdot T_h^u \boldsymbol{\lambda}_{H,h}, \nabla \cdot \boldsymbol{w})_\tau.
\end{aligned} \tag{41}$$

Moreover, using similar arguments as above, we can prove that:

$$\begin{aligned}
\int_K \hat{T}^p \boldsymbol{f} dx &= \int_K \hat{T}_h^p \boldsymbol{f} dx + \frac{1}{2}\big(\nabla(\hat{T}^u \boldsymbol{f} - \hat{T}_h^u \boldsymbol{f})\boldsymbol{\alpha}, \boldsymbol{w}\big)_K - \frac{1}{2}(\hat{T}^u \boldsymbol{f} - \hat{T}_h^u \boldsymbol{f}, (\nabla \boldsymbol{w})\boldsymbol{\alpha})_K + (\gamma_0\,(\hat{T}^u \boldsymbol{f} - \hat{T}_h^u \boldsymbol{f}), \boldsymbol{w})_K \\
&\quad + \sum_{\tau \in \mathcal{T}_h^K} \delta_\tau(-\nu\Delta \hat{T}_h^u \boldsymbol{f} + (\nabla \hat{T}_h^u \boldsymbol{f})\boldsymbol{\alpha} + \gamma \hat{T}_h^u \boldsymbol{f} + \nabla \hat{T}_h^p \boldsymbol{f} - \boldsymbol{f}, -(\nabla \boldsymbol{w})\boldsymbol{\alpha} + \gamma \boldsymbol{w})_\tau - \sum_{\tau \in \mathcal{T}_h^K} \kappa_\tau(\nabla \cdot \hat{T}_h^u \boldsymbol{f}, \nabla \cdot \boldsymbol{w})_\tau.
\end{aligned} \tag{42}$$

Note th at from the definition of $\boldsymbol{w}$ we have that $\|\boldsymbol{w}\|_{1,\Omega}$ is a constant depending only on the domain Ω and the dimension d. Now, from the second equation of (20), (41), (42), and Lemma 3, we get:

$$
\begin{aligned}
\int_\Omega T^p(\boldsymbol{\lambda}-\boldsymbol{\lambda}_{H,h})dx &= \sum_{K\in\mathscr{T}_H}\left(\int_K T^p\boldsymbol{\lambda}dx - \int_K T^p\boldsymbol{\lambda}_{H,h}\,dx\right) = \sum_{K\in\mathscr{T}_H}\left(-\int_K \hat{T}^p\boldsymbol{f}dx - \int_K T^p\boldsymbol{\lambda}_{H,h}\,dx\right)\\
&= \sum_{K\in\mathscr{T}_H}\Bigg(-\int_K \hat{T}_h^p\boldsymbol{f}dx - \frac{1}{2}\big(\nabla(\hat{T}^u\boldsymbol{f}-\hat{T}_h^u\boldsymbol{f})\boldsymbol{\alpha},\boldsymbol{w}\big)_K + \frac{1}{2}(\hat{T}^u\boldsymbol{f}-\hat{T}_h^u\boldsymbol{f},(\nabla\boldsymbol{w})\boldsymbol{\alpha})_K - (\gamma_0\,(\hat{T}^u\boldsymbol{f}-\hat{T}_h^u\boldsymbol{f}),\boldsymbol{w})_K\\
&\quad - \sum_{\tau\in\mathscr{T}_h^K}\delta_\tau(-\nu\Delta\hat{T}_h^u\boldsymbol{f}+(\nabla\hat{T}_h^u\boldsymbol{f})\boldsymbol{\alpha}+\gamma\hat{T}_h^u\boldsymbol{f}+\nabla\hat{T}_h^p\boldsymbol{f}-\boldsymbol{f},-(\nabla\boldsymbol{w})\boldsymbol{\alpha}+\gamma\boldsymbol{w})_\tau + \sum_{\tau\in\mathscr{T}_h^K}\kappa_\tau(\nabla\cdot\hat{T}_h^u\boldsymbol{f},\nabla\cdot\boldsymbol{w})_\tau\\
&\quad -\int_K T_h^p\boldsymbol{\lambda}_{H,h}dx - \frac{1}{2}\big(\nabla(T^u\boldsymbol{\lambda}_H - T_h^u\boldsymbol{\lambda}_{H,h})\boldsymbol{\alpha},\boldsymbol{w}\big)_K + \frac{1}{2}(T^u\boldsymbol{\lambda}_H - T_h^u\boldsymbol{\lambda}_{H,h},(\nabla\boldsymbol{w})\boldsymbol{\alpha})_K - (\gamma_0\,(T^u\boldsymbol{\lambda}_H - T_h^u\boldsymbol{\lambda}_{H,h}),\boldsymbol{w})_K\\
&\quad - \sum_{\tau\in\mathscr{T}_h^K}\delta_\tau(-\nu\Delta T_h^u\boldsymbol{\lambda}_{H,h}+(\nabla T_h^u\boldsymbol{\lambda}_{H,h})\boldsymbol{\alpha}+\gamma T_h^u\boldsymbol{\lambda}_{H,h}+\nabla T_h^p\boldsymbol{\lambda}_{H,h},-(\nabla\boldsymbol{w})\boldsymbol{\alpha}+\gamma\boldsymbol{w})_\tau + \sum_{\tau\in\mathscr{T}_h^K}\kappa_\tau(\nabla\cdot T_h^u\boldsymbol{\lambda}_{H,h},\nabla\cdot\boldsymbol{w})_\tau\Bigg)\\
&= \sum_{K\in\mathscr{T}_H}\Bigg(-\frac{1}{2}\nabla(\boldsymbol{u}_H-\boldsymbol{u}_{H,h})\boldsymbol{\alpha},\boldsymbol{w})_K + \frac{1}{2}(\boldsymbol{u}_H-\boldsymbol{u}_{H,h},(\nabla\boldsymbol{w})\boldsymbol{\alpha})_K - (\gamma_0(\boldsymbol{u}_H-\boldsymbol{u}_{H,h}),\boldsymbol{w})_K\\
&\quad + \sum_{\tau\in\mathscr{T}_h^K}\delta_\tau(\nu\Delta\boldsymbol{u}_{H,h}-(\nabla\boldsymbol{u}_{H,h})\alpha-\gamma\boldsymbol{u}_{H,h}-\nabla p_{H,h}-\boldsymbol{f},-(\nabla\boldsymbol{w})\boldsymbol{\alpha}+\gamma\boldsymbol{w})_\tau + \sum_{\tau\in\mathscr{T}_h^K}\kappa_\tau(\nabla\cdot\boldsymbol{u}_{H,h},\nabla\cdot\boldsymbol{w})_\tau\Bigg)\\
&\preceq \sum_{K\in\mathscr{T}_H}\Bigg(|\boldsymbol{u}_H-\boldsymbol{u}_{H,h}|_{1,K}\|\boldsymbol{\alpha}\|_{\infty,K}\|\boldsymbol{w}\|_{0,K} + \|\boldsymbol{u}_H-\boldsymbol{u}_{H,h}\|_{0,K}|\boldsymbol{w}|_{1,K}\|\boldsymbol{\alpha}\|_{\infty,K} + \|\gamma_0\|_{\infty,K}\|\boldsymbol{u}_H-\boldsymbol{u}_{H,h}\|_{0,K}\|\boldsymbol{w}\|_{0,K}\\
&\quad + \|\boldsymbol{\alpha}\|_{\infty,K}\sum_{\tau\in\mathscr{T}_h^K}\delta_\tau\|\boldsymbol{R}_\tau^K\|_{0,\tau}|\boldsymbol{w}|_{1,\tau} + \gamma\sum_{\tau\in\mathscr{T}_h^K}\delta_\tau\|\boldsymbol{R}_\tau^K\|_{0,\tau}\|\boldsymbol{w}\|_{1,\tau} + \sum_{\tau\in\mathscr{T}_h^K}\kappa_\tau\|\nabla\cdot\boldsymbol{u}_{H,h}\|_{0,\tau}\,|\boldsymbol{w}|_{1,\tau}\Bigg)\\
&\preceq \sum_{K\in\mathscr{T}_H}\Bigg(|\boldsymbol{u}_H-\boldsymbol{u}_{H,h}|_{1,K}\|\boldsymbol{\alpha}\|_{\infty,K}\,\|\boldsymbol{w}\|_{1,K} + \|\boldsymbol{u}_H-\boldsymbol{u}_{H,h}\|_{0,K}|\boldsymbol{w}|_{1,K}\|\boldsymbol{\alpha}\|_{\infty,K}\\
&\quad + \|\gamma_0\|_{\infty,K}\|\boldsymbol{u}_H-\boldsymbol{u}_{H,h}\|_{0,K}\,\|\boldsymbol{w}\|_{1,K} + \|\boldsymbol{\alpha}\|_{\infty,K}\left(\sum_{\tau\in\mathscr{T}_h^K}\delta_\tau\|\boldsymbol{R}_\tau^K\|_{0,\tau}^2\right)^{1/2}\left(\sum_{\tau\in\mathscr{T}_h^K}\delta_\tau|\boldsymbol{w}|_{1,\tau}^2\right)^{1/2}\\
&\quad + \gamma\left(\sum_{\tau\in\mathscr{T}_h^K}\delta_\tau\|\boldsymbol{R}_\tau^K\|_{0,\tau}^2\right)^{1/2}\left(\sum_{\tau\in\mathscr{T}_h^K}\delta_\tau\|\boldsymbol{w}\|_{0,\tau}^2\right)^{1/2} + \left(\sum_{\tau\in\mathscr{T}_h^K}\kappa_\tau\|\nabla\cdot\boldsymbol{u}_{H,h}\|_{0,\tau}^2\right)^{1/2}\left(\sum_{\tau\in\mathscr{T}_h^K}\kappa_\tau\|\boldsymbol{w}\|_{1,\tau}^2\right)^{1/2}\Bigg)\\
&\preceq \sum_{K\in\mathscr{T}_H}\Bigg(|\boldsymbol{u}_H-\boldsymbol{u}_{H,h}|_{1,K}\|\boldsymbol{\alpha}\|_{\infty,K}\,\|\boldsymbol{w}\|_{1,K} + \|\boldsymbol{u}_H-\boldsymbol{u}_{H,h}\|_{0,K}|\boldsymbol{w}|_{1,K}\|\boldsymbol{\alpha}\|_{\infty,K} + \|\gamma_0\|_{\infty,K}\|\boldsymbol{u}_H-\boldsymbol{u}_{H,h}\|_{0,K}\,\|\boldsymbol{w}\|_{1,K}\\
&\quad + \left(\sum_{\tau\in\mathscr{T}_h^K}\delta_\tau\|\boldsymbol{R}_\tau^K\|_{0,\tau}^2\right)^{1/2}|\boldsymbol{w}|_{1,K} + \left(\sum_{\tau\in\mathscr{T}_h^K}\delta_\tau\|\boldsymbol{R}_\tau^K\|_{0,\tau}^2\right)^{1/2}\|\boldsymbol{w}\|_{1,K} + \left(\sum_{\tau\in\mathscr{T}_h^K}\kappa_\tau\|\nabla\cdot\boldsymbol{u}_{H,h}\|_{0,\tau}^2\right)^{1/2}\|\boldsymbol{w}\|_{1,K}\Bigg)\\
&\preceq \eta_2.
\end{aligned} \tag{43}
$$

Now, define $\boldsymbol{\mu} := \boldsymbol{\lambda} - \boldsymbol{\lambda}_{H,h}$ and $T^p\boldsymbol{\mu} := T^p\boldsymbol{\lambda} - T^p\boldsymbol{\lambda}_{H,h}$. Using the orthogonal decomposition $T^p\boldsymbol{\mu} = \tilde{p} + p_0$, where $\tilde{p} \in L_0^2(\Omega)$ and $p_0 := \dfrac{1}{|\Omega|}\displaystyle\int_\Omega T^p\boldsymbol{\mu}$, there exists $\tilde{\boldsymbol{w}} \in H_0^1(\Omega)^d$ (see [26]) with $\nabla\cdot\tilde{\boldsymbol{w}} = \tilde{p}$ in Ω and $|\tilde{\boldsymbol{w}}|_{1,\Omega} \le C\|\tilde{p}\|_{0,\Omega}$, where $C > 0$ is independent of H and h. From (17), it holds:

$$
a(T^u\boldsymbol{\mu},\tilde{\boldsymbol{w}}) + b(\tilde{\boldsymbol{w}},T^p\boldsymbol{\mu}) = -(\mu,\tilde{\boldsymbol{w}})_{\mathscr{T}_H} = 0. \tag{44}
$$

Hence, using (43) and (44), we have that:

$$\begin{aligned}
\|T^p\boldsymbol{\mu}\|_Q^2 &= (T^p\boldsymbol{\mu}, T^p\boldsymbol{\mu})_\Omega = (T^p\boldsymbol{\mu}, \tilde{p})_\Omega + (T^p\boldsymbol{\mu}, p_0)_\Omega = (T^p\boldsymbol{\mu}, \nabla\cdot\tilde{\boldsymbol{w}})_\Omega + (T^p\boldsymbol{\mu}, p_0)_\Omega \\
&= -b(\tilde{\boldsymbol{w}}, T^p\boldsymbol{\mu}) + (T^p\boldsymbol{\mu}, p_0)_\Omega = a(T^u\boldsymbol{\mu}, \tilde{\boldsymbol{w}}) + (T^p\boldsymbol{\mu}, p_0)_\Omega \\
&= \nu(\nabla T^u\boldsymbol{\mu}, \nabla\tilde{\boldsymbol{w}})_\Omega + \frac{1}{2}((\nabla T^u\boldsymbol{\mu})\boldsymbol{\alpha}, \tilde{\boldsymbol{w}})_\Omega - \frac{1}{2}(T^u\boldsymbol{\mu}, (\nabla\tilde{\boldsymbol{w}})\boldsymbol{\alpha})_\Omega + (\gamma_0 T^u\boldsymbol{\mu}, \tilde{\boldsymbol{w}})_\Omega + (T^p\boldsymbol{\mu}, p_0)_\Omega \\
&\preceq |T^u\boldsymbol{\mu}|_{1,\Omega}|\tilde{\boldsymbol{w}}|_{1,\Omega} + |T^u\boldsymbol{\mu}|_{1,\Omega}\|\boldsymbol{\alpha}\|_{\infty,\Omega}\|\tilde{\boldsymbol{w}}\|_{0,\Omega} + \|T^u\boldsymbol{\mu}\|_{0,\Omega}\|\boldsymbol{\alpha}\|_{\infty,\Omega}|\tilde{\boldsymbol{w}}|_{1,\Omega} + \|\gamma_0\|_{\infty,\Omega}\|T^u\boldsymbol{\mu}\|_{1,\Omega}\|\tilde{\boldsymbol{w}}\|_{1,\Omega} \\
&\quad + \|T^p\boldsymbol{\mu}\|_{0,\Omega}\|p_0\|_{0,\Omega} \\
&\preceq (\|T^u\boldsymbol{\mu}\|_{\mathbf{V}} + \|p_0\|_{0,\Omega})\|T^p\boldsymbol{\mu}\|_Q \\
&\preceq (\|T^u\boldsymbol{\mu}\|_{\mathbf{V}} + \eta_2)\|T^p\boldsymbol{\mu}\|_Q,
\end{aligned}$$

we conclude that:

$$\|T^p\boldsymbol{\mu}\|_Q \preceq \|T^u\boldsymbol{\mu}\|_{\mathbf{V}} + \eta_2,$$

and the result follows. □

Lemma 5 *Let $\boldsymbol{\lambda}$ and $\boldsymbol{\lambda}_{H,h}$ be the solutions of (20) and (24), respectively. Then we have:*

$$\|T^u(\boldsymbol{\lambda} - \boldsymbol{\lambda}_{H,h})\|_{\mathbf{V}} \preceq \eta.$$

Proof Let $\boldsymbol{\mu} := \boldsymbol{\lambda} - \boldsymbol{\lambda}_{H,h}$. We notice from (17) and (22) that:

$$\begin{aligned}
-(\boldsymbol{\mu}, T^u\boldsymbol{\mu})_{\partial\mathscr{T}_H} &= \sum_{K\in\mathscr{T}_H} B_K((T^u\boldsymbol{\mu}, T^p\boldsymbol{\mu}), (T^u\boldsymbol{\mu}, T^p\boldsymbol{\mu})) \\
&= \sum_{K\in\mathscr{T}_H} \nu(\nabla T^u\boldsymbol{\mu}, \nabla T^u\boldsymbol{\mu})_K + \gamma_0(T^u\boldsymbol{\mu}, T^u\boldsymbol{\mu})_K \\
&\geq C_1\|T^u\boldsymbol{\mu}\|_{\mathbf{V}}^2. \qquad (45)
\end{aligned}$$

Now, combining (6) and (17), we find that:

$$\begin{aligned}
\frac{\sqrt{2}}{2}\|\boldsymbol{\mu}\|_{\boldsymbol{\Lambda}} &\leq \sup_{\boldsymbol{v}\in\mathbf{V}} \frac{-\sum_{K\in\mathscr{T}_H} B_K((T^u\boldsymbol{\mu}, T^p\boldsymbol{\mu}), (\boldsymbol{v}, 0))}{\|\boldsymbol{v}\|_{\mathbf{V}}} \\
&= \sup_{\boldsymbol{v}\in\mathbf{V}} \frac{-\sum_{K\in\mathscr{T}_H}\left[a_K(T^u\boldsymbol{\mu}, \boldsymbol{v}) + b_K(\boldsymbol{v}, T^p\boldsymbol{\mu})\right]}{\|\boldsymbol{v}\|_{\mathbf{V}}} \\
&\preceq (\|T^u\boldsymbol{\mu}\|_{\mathbf{V}} + \|T^p\boldsymbol{\mu}\|_Q),
\end{aligned}$$

and using Lemma 4, we get:

$$\|\boldsymbol{\mu}\|_{\boldsymbol{\Lambda}} \preceq \|T^u\boldsymbol{\mu}\|_{\mathbf{V}} + \eta_2. \qquad (46)$$

According to Lemma 4.2 in [11], there exists $\boldsymbol{\chi} \in \mathbf{V}$ satisfying:

$$(\boldsymbol{\mu}, \boldsymbol{\chi})_{\partial\mathscr{T}_H} = \langle\boldsymbol{\mu}, \boldsymbol{g}\rangle_{\partial\Omega} - (\boldsymbol{\mu}, \boldsymbol{u}_{H,h})_{\partial\mathscr{T}_H} \quad \text{for all } \boldsymbol{\mu} \in \boldsymbol{\Lambda},$$

and

$$\|\boldsymbol{\chi}\|_{\mathbf{V}} \preceq \eta_1.$$

Then, using this result, (8), (32), (45), (46), and Lemma 3, we obtain:

$$
\begin{aligned}
C_1 \|T^u \boldsymbol{\mu}\|_{\mathbf{V}}^2 \leq -(\boldsymbol{\mu}, T^u \boldsymbol{\mu})_{\partial \mathscr{T}_H} &= -(\boldsymbol{\mu}, T^u \boldsymbol{\lambda} - T^u \boldsymbol{\lambda}_{H,h})_{\partial \mathscr{T}_H} \\
&= -(\boldsymbol{\mu}, T^u \boldsymbol{\lambda} + \hat{T}^u \boldsymbol{f} - (T^u \boldsymbol{\lambda}_{H,h} + \hat{T}^u \boldsymbol{f}))_{\partial \mathscr{T}_H} \\
&= -\langle \boldsymbol{\mu}, \boldsymbol{g} \rangle_{\partial\Omega} + (\boldsymbol{\mu}, T^u \boldsymbol{\lambda}_{H,h} + \hat{T}^u \boldsymbol{f})_{\partial \mathscr{T}_H} \\
&= -\langle \boldsymbol{\mu}, \boldsymbol{g} \rangle_{\partial\Omega} + (\boldsymbol{\mu}, \boldsymbol{u}_{H,h})_{\partial \mathscr{T}_H} + (\boldsymbol{\mu}, \boldsymbol{u}_H - \boldsymbol{u}_{H,h})_{\partial \mathscr{T}_H} \\
&= -(\boldsymbol{\mu}, \boldsymbol{\chi})_{\partial \mathscr{T}_H} + (\boldsymbol{\mu}, \boldsymbol{u}_H - \boldsymbol{u}_{H,h})_{\partial \mathscr{T}_H} \\
&\leq \|\boldsymbol{\mu}\|_{\boldsymbol{\Lambda}} (\|\boldsymbol{\chi}\|_{\mathbf{V}} + \|\boldsymbol{u}_H - \boldsymbol{u}_{H,h}\|_{\mathbf{V}}) \\
&\leq C_2 \|\boldsymbol{\mu}\|_{\boldsymbol{\Lambda}} (\eta_1 + \eta_2) \\
&\leq C_2 (\|T^u \boldsymbol{\mu}\|_{\mathbf{V}} + \eta_2)(\eta_1 + \eta_2) \\
&\leq C_2\, \eta \|T^u \boldsymbol{\mu}\|_{\mathbf{V}} + C_2\, \eta^2.
\end{aligned}
$$

Now, using the inequality (45) and the inequality $ab \leq \dfrac{\delta}{2} a^2 + \dfrac{1}{2\delta} b^2$ with $\delta > \dfrac{C_2}{2C_1}$, we arrive at:

$$
\|T^u \boldsymbol{\mu}\|_{\mathbf{V}} \preceq \eta, \tag{47}
$$

and we conclude the result.

□

Theorem 5 *Let $(\boldsymbol{u}, p)$ and $(\boldsymbol{u}_H, p_H)$ be the solutions of (21) and (35), respectively. Then we have:*

$$
\|(\boldsymbol{u} - \boldsymbol{u}_H, p - p_H)\|_{\mathbf{V} \times Q} \preceq \eta. \tag{48}
$$

Proof Using Lemmas 4 and 5, the result follows. □

4.2 Local efficiency and reliability analysis

Before we state the main result of this work, we need first an auxiliary result.

Theorem 6 *Let $K \in \mathscr{T}_H$. For each $\tau \in \mathscr{T}_h^K$, there holds:*

$$
h_\tau \|\boldsymbol{R}_\tau^K\|_{0,\tau} \preceq \left[h_\tau \|\boldsymbol{u} - \boldsymbol{u}_{H,h}\|_{0,\tau} + (1 + h_\tau) |\boldsymbol{u} - \boldsymbol{u}_{H,h}|_{1,\tau} + \|p - p_{H,h}\|_{0,\tau} \right], \tag{49}
$$

and

$$
\|\nabla \cdot \boldsymbol{u}_{H,h}\|_{0,\tau} \preceq |\boldsymbol{u} - \boldsymbol{u}_{H,h}|_{1,\tau}.
$$

Furthermore, for each $\zeta \in \mathscr{E}_0^K$, we have:

$$
h_\zeta^{1/2} \|\boldsymbol{R}_\zeta^K\|_{0,\zeta} \preceq \sum_{\tau \in \omega_\zeta} \left[|\boldsymbol{u} - \boldsymbol{u}_{H,h}|_{1,\tau} + \|\boldsymbol{u} - \boldsymbol{u}_{H,h}\|_{0,\tau} + \|p - p_{H,h}\|_{0,\tau} \right],
$$

and for all $\zeta \in \mathscr{E}_b^K$, there holds:

$$
h_\zeta^{1/2} \|\boldsymbol{R}_\zeta^K\|_{0,\zeta} \preceq \sum_{\tau \in \omega_\zeta} \left[|\boldsymbol{u} - \boldsymbol{u}_{H,h}|_{1,\tau} + \|\boldsymbol{u} - \boldsymbol{u}_{H,h}\|_{0,\tau} + \|p - p_{H,h}\|_{0,\tau} \right] + \|\boldsymbol{\lambda} - \boldsymbol{\lambda}_H\|_{-\frac{1}{2},\partial K}. \tag{50}
$$

Proof We define $\boldsymbol{b}_\tau^K := b_\tau^K \boldsymbol{R}_\tau^K$ and $\boldsymbol{b}_\zeta^K := b_\zeta^K \boldsymbol{P}_\zeta^K(\boldsymbol{R}_\zeta^K)$. Using integration by parts and Theorem 2, we arrive at:

$$\begin{aligned}
(\boldsymbol{R}_\tau^K, \boldsymbol{b}_\tau^K)_\tau &= \left(\nu\Delta\boldsymbol{u}_{H,h} - (\nabla\boldsymbol{u}_{H,h})\boldsymbol{\alpha} - \gamma\boldsymbol{u}_{H,h} - \nabla p_{H,h} + \boldsymbol{f}, \boldsymbol{b}_\tau^K\right)_\tau \\
&= \left(\nu\Delta(\boldsymbol{u}_{H,h} - \boldsymbol{u}) - (\nabla(\boldsymbol{u}_{H,h} - \boldsymbol{u}))\boldsymbol{\alpha} - \gamma(\boldsymbol{u}_{H,h} - \boldsymbol{u}) - \nabla(p_{H,h} - p), \boldsymbol{b}_\tau^K\right)_\tau \\
&\leq \nu|\boldsymbol{u} - \boldsymbol{u}_{H,h}|_{1,\tau}|\boldsymbol{b}_\tau^K|_{1,\tau} + |\boldsymbol{u} - \boldsymbol{u}_{H,h}|_{1,\tau}\|\boldsymbol{\alpha}\|_\infty\|\boldsymbol{b}_\tau^K\|_{0,\tau} + \gamma\|\boldsymbol{u} - \boldsymbol{u}_{H,h}\|_{0,\tau}\|\boldsymbol{b}_\tau^K\|_{0,\tau} \\
&\quad + \sqrt{d}\|p - p_{H,h}\|_{0,\tau}|\boldsymbol{b}_\tau^K|_{1,\tau} \\
&\preceq \left((1 + h_\tau^{-1})|\boldsymbol{u} - \boldsymbol{u}_{H,h}|_{1,\tau} + \|\boldsymbol{u} - \boldsymbol{u}_{H,h}\|_{0,\tau} + h_\tau^{-1}\|p - p_{H,h}\|_{0,\tau}\right)\|\boldsymbol{R}_\tau^K\|_{0,\tau},
\end{aligned}$$

and then:

$$h_\tau\|\boldsymbol{R}_\tau^K\|_{0,\tau} \preceq \left[h_\tau\|\boldsymbol{u} - \boldsymbol{u}_{H,h}\|_{0,\tau} + (1 + h_\tau)|\boldsymbol{u} - \boldsymbol{u}_{H,h}|_{1,\tau} + \|p - p_{H,h}\|_{0,\tau}\right].$$

Again, by Theorem 2, we obtain that:

$$\begin{aligned}
\|\nabla\cdot\boldsymbol{u}_{H,h}\|_{0,\tau}^2 &\preceq (\nabla\cdot\boldsymbol{u}_{H,h}, b_\tau^K\nabla\cdot\boldsymbol{u}_{H,h})_\tau \\
&\preceq (\nabla\cdot\boldsymbol{u}_{H,h}, b_\tau^K\nabla\cdot\boldsymbol{u}_{H,h})_\Omega \\
&\preceq (\nabla\cdot(\boldsymbol{u}_{H,h} - \boldsymbol{u}), b_\tau^K\nabla\cdot\boldsymbol{u}_{H,h})_\Omega \\
&\preceq |\boldsymbol{u}_{H,h} - \boldsymbol{u}|_{1,\tau}\|\nabla\cdot\boldsymbol{u}_{H,h}\|_{0,\tau},
\end{aligned}$$

and therefore:

$$\|\nabla\cdot\boldsymbol{u}_{H,h}\|_{0,\tau} \preceq |\boldsymbol{u}_{H,h} - \boldsymbol{u}|_{1,\tau}.$$

Let $\zeta \in \mathscr{E}_0^K$. From Lemma 2 and Theorem 2, we find that:

$$\begin{aligned}
(\boldsymbol{R}_\zeta^K, \boldsymbol{b}_\zeta^K)_\zeta &= \boldsymbol{R}_h^K(\boldsymbol{b}_\zeta^K) - \sum_{\tau\in\omega_\zeta}(\boldsymbol{R}_\tau^K, \boldsymbol{b}_\zeta^K)_\tau \\
&\preceq \sum_{\tau\in\omega_\zeta}\Big[|\boldsymbol{u} - \boldsymbol{u}_{H,h}|_{1,\tau}|\boldsymbol{b}_\zeta^K|_{1,\tau} + \|\boldsymbol{u} - \boldsymbol{u}_{H,h}\|_{0,\tau}\|\boldsymbol{b}_\zeta^K\|_{0,\tau} + |\boldsymbol{u} - \boldsymbol{u}_{H,h}|_{1,\tau}\|\boldsymbol{b}_\zeta^K\|_{0,\tau} + \\
&\quad \|p - p_{H,h}\|_{0,\tau}|\boldsymbol{b}_\zeta^K|_{1,\tau} + \|\boldsymbol{R}_\tau^K\|_{0,\tau}\|\boldsymbol{b}_\zeta^K\|_{0,\tau}\Big] \\
&\preceq \sum_{\tau\in\omega_\zeta}\Big[h_\tau^{-1/2}|\boldsymbol{u} - \boldsymbol{u}_{H,h}|_{1,\tau} + h_\tau^{1/2}\|\boldsymbol{u} - \boldsymbol{u}_{H,h}\|_{0,\tau} + h_\tau^{1/2}|\boldsymbol{u} - \boldsymbol{u}_{H,h}|_{1,\tau} + \\
&\quad h_\tau^{-1/2}\|p - p_{H,h}\|_{0,\tau} + h_\tau^{1/2}\|\boldsymbol{R}_\tau^K\|_{0,\tau}\Big]\|\boldsymbol{R}_\zeta^K\|_{0,\zeta},
\end{aligned}$$

thus using Theorem 2, (49) and the regularity of the second-level meshes, we get:

$$\begin{aligned}
h_\zeta^{1/2}\|\boldsymbol{R}_\zeta^K\|_{0,\zeta} &\preceq \sum_{\tau\in\omega_\zeta}\left[(1 + h_\tau)|\boldsymbol{u} - \boldsymbol{u}_{H,h}|_{1,\tau} + (1 + h_\tau)\|\boldsymbol{u} - \boldsymbol{u}_{H,h}\|_{0,\tau} + \|p - p_{H,h}\|_{0,\tau}\right] \\
&\preceq \sum_{\tau\in\omega_\zeta}\left[|\boldsymbol{u} - \boldsymbol{u}_{H,h}|_{1,\tau} + \|\boldsymbol{u} - \boldsymbol{u}_{H,h}\|_{0,\tau} + \|p - p_{H,h}\|_{0,\tau}\right].
\end{aligned}$$

Next, let $\zeta \in \mathscr{E}_b^K$. Using Theorem 2 and the regularity of the partition $\mathscr{T}_h^K$, we arrive at:

$$\|\boldsymbol{b}_\zeta^K\|_{1,\tau} \preceq \sqrt{h_\tau + h_\tau^{-1}}\,\|\boldsymbol{R}_\zeta^K\|_{0,\zeta} \preceq h_\zeta^{-1/2}\|\boldsymbol{R}_\zeta^K\|_{0,\zeta}.$$

Now consider:

$$a_K(\boldsymbol{u},\boldsymbol{v}) + b_K(\boldsymbol{v},p) = \sum_{\tau\in\mathscr{T}_h^K}\Big(a_\tau(\boldsymbol{u},\boldsymbol{v}) + b_\tau(\boldsymbol{v},p)\Big),$$

where $a_\tau(\cdot,\cdot) = a_K(\cdot,\cdot)\Big|_\tau$ and $b_\tau(\cdot,\cdot) = b_K(\cdot,\cdot)\Big|_\tau$. Using again Lemma 2, Theorem 2, (49), (15), and the regularity of the meshes of the second level, it holds:

$$\begin{aligned}
(\boldsymbol{R}_\zeta^K,\boldsymbol{b}_\zeta^K)_\zeta &= \boldsymbol{R}_h^K(\boldsymbol{b}_\zeta^K) - \sum_{\tau\in\omega_\zeta}(\boldsymbol{R}_\tau^K,\boldsymbol{b}_\zeta^K)_\tau\\
&= a_K(\boldsymbol{u}-\boldsymbol{u}_{H,h},\boldsymbol{b}_\zeta^K) + b_K(\boldsymbol{b}_\zeta^K, p-p_{H,h}) + \langle\boldsymbol{\lambda}-\boldsymbol{\lambda}_H,\boldsymbol{b}_\zeta^K\rangle_{\partial K} - \sum_{\tau\in\omega_\zeta}(\boldsymbol{R}_\tau^K,\boldsymbol{b}_\zeta^K)_\tau\\
&= \sum_{\tau\in\omega_\zeta}\Big(a_\tau(\boldsymbol{u}-\boldsymbol{u}_{H,h},\boldsymbol{b}_\zeta^K) + b_\tau(\boldsymbol{b}_\zeta^K,p-p_{H,h}) - (\boldsymbol{R}_\tau^K,\boldsymbol{b}_\zeta^K)_\tau\Big) + \langle\boldsymbol{\lambda}-\boldsymbol{\lambda}_H,\boldsymbol{b}_\zeta^K\rangle_{\partial K}\\
&\preceq \sum_{\tau\in\omega_\zeta}\Big(|\boldsymbol{u}-\boldsymbol{u}_{H,h}|_{1,\tau} + \|\boldsymbol{u}-\boldsymbol{u}_{H,h}\|_{0,\tau} + \|p-p_{H,h}\|_{0,\tau}\Big)h_\zeta^{-1/2}\|\boldsymbol{R}_\zeta^K\|_{0,\zeta} + \|\boldsymbol{\lambda}-\boldsymbol{\lambda}_H\|_{-\frac{1}{2},\partial K}\|\boldsymbol{b}_\zeta^K\|_{\frac{1}{2},\partial K}\\
&\preceq \sum_{\tau\in\omega_\zeta}\Big(|\boldsymbol{u}-\boldsymbol{u}_{H,h}|_{1,\tau} + \|\boldsymbol{u}-\boldsymbol{u}_{H,h}\|_{0,\tau} + \|p-p_{H,h}\|_{0,\tau}\Big)h_\zeta^{-1/2}\|\boldsymbol{R}_\zeta^K\|_{0,\zeta} + \|\boldsymbol{\lambda}-\boldsymbol{\lambda}_H\|_{-\frac{1}{2},\partial K}\,h_\zeta^{-1/2}\|\boldsymbol{R}_\zeta^K\|_{0,\zeta},
\end{aligned}$$

thus, we get (50). □

To present the main result, we need to define the following discrete norm for the velocity:

$$\|\boldsymbol{v}\|_{\mathbf{V},\omega_F} := \left\{\sum_{K\in\omega_F}\left[H_K^{-2}\|\boldsymbol{v}\|_{0,K}^2 + |\boldsymbol{v}|_{1,K}^2\right]\right\}^{1/2},$$

for all $F \in \mathscr{E}_H$.

We are now in position to establish the results that show the efficiency and reliatibity of the error estimator η.

Theorem 7 (Main Result) *Let $(\boldsymbol{u},p) \in \mathbf{V}\times Q$ the continuous solution of MHM method and $(\boldsymbol{u}_{H,h}, p_{h,h}) \in \mathbf{V}_h \times Q_h$ the discrete solution of two-level MHM method, given in* (21) *and* (32)*, and with $\boldsymbol{\lambda}$ and $\boldsymbol{\lambda}_{H,h}$ solutions of* (20) *and* (24) *respectively. Then:*

$$\|\boldsymbol{u}-\boldsymbol{u}_{H,h}\|_{\mathbf{V}} + \|p-p_{H,h}\|_Q + \|\boldsymbol{\lambda}-\boldsymbol{\lambda}_{H,h}\|_{\boldsymbol{\Lambda}} \preceq \eta.$$

Moreover, given $F \in \mathscr{E}_H$, we have:

$$\eta_{1,F} \preceq \|\boldsymbol{u}-\boldsymbol{u}_{H,h}\|_{\mathbf{V},\omega_F},$$

and

$$\eta_{2,K} \preceq \|\boldsymbol{u}-\boldsymbol{u}_{H,h}\|_{\mathbf{V}(K)} + \|p-p_{H,h}\|_{Q(K)} + \|\boldsymbol{\lambda}-\boldsymbol{\lambda}_{H,h}\|_{-\frac{1}{2},\partial K}, \tag{51}$$

for all $K \in \mathscr{T}_H$.

Proof Applying Lemma 3, (48) and the triangular inequality, we get:

$$\|(\boldsymbol{u}-\boldsymbol{u}_{H,h}, p-p_{H,h})\|_{\mathbf{V}\times Q} \le \|(\boldsymbol{u}-\boldsymbol{u}_{H}, p-p_{H})\|_{\mathbf{V}\times Q} + \|(\boldsymbol{u}_H-\boldsymbol{u}_{H,h}, p_H-p_{H,h})\|_{\mathbf{V}\times Q} \preceq \eta.$$

Now, using (46) and (47) we get:

$$\|\boldsymbol{\lambda}-\boldsymbol{\lambda}_{H,h}\|_{\boldsymbol{\Lambda}} \preceq \eta.$$

On the other hand, since $\boldsymbol{R}_F \in L^2(F)^d$, then:

$$\|\boldsymbol{R}_F\|_{0,F}^2 = \frac{1}{2}(\boldsymbol{R}_F, [\![\boldsymbol{u}-\boldsymbol{u}_{H,h}]\!])_F \le \frac{1}{2}\|\boldsymbol{R}_F\|_{0,F}\| [\![\boldsymbol{u}-\boldsymbol{u}_{H,h}]\!] \|_{0,F},$$

and by Lemma 1, we arrive to:

$$\|\boldsymbol{R}_F\|_{0,F} \preceq H_F^{1/2} \sum_{K\in\omega_F}\left(H_K^{-2}\|\boldsymbol{u}-\boldsymbol{u}_{H,h}\|_{0,K}^2 + |\boldsymbol{u}-\boldsymbol{u}_{H,h}|_{1,K}^2\right)^{1/2} \preceq H_F^{1/2}\|\boldsymbol{u}-\boldsymbol{u}_{H,h}\|_{\mathbf{V},\omega_F}.$$

Finally, using the definition (33) of $\eta_{2,K}$ and Theorem 6, we arrive at:

$$\begin{aligned}
\eta_{2,K} &\preceq \sum_{\tau\in\mathscr{T}_h^K}\left[h_\tau\|\boldsymbol{R}_\tau^K\|_{0,\tau} + \|\nabla\cdot\boldsymbol{u}_{H,h}\|_{0,\tau}\right] + \sum_{\zeta\in\mathscr{E}_h^K} h_\zeta^{1/2}\|\boldsymbol{R}_\zeta^K\|_{0,\zeta} \\
&\preceq \left[\|\boldsymbol{u}-\boldsymbol{u}_{H,h}\|_{0,K} + |\boldsymbol{u}-\boldsymbol{u}_{H,h}|_{1,K} + \|p-p_{H,h}\|_{0,K}\right] + \|\boldsymbol{\lambda}-\boldsymbol{\lambda}_H\|_{-\frac{1}{2},\partial K} \\
&\preceq \|(\boldsymbol{u}-\boldsymbol{u}_{H,h}, p-p_{H,h})\|_{\mathbf{V}(K)\times Q(K)} + \|\boldsymbol{\lambda}-\boldsymbol{\lambda}_H\|_{-\frac{1}{2},\partial K},
\end{aligned}$$

which finishes the proof. □

Remark 8 If we assume that $\boldsymbol{\lambda} \in L^2(\partial\mathscr{T}_H)$, then it is easy to prove that we can modify (51) as follows:

$$\eta_{2,K} \preceq \|(\boldsymbol{u}-\boldsymbol{u}_{H,h}, p-p_{H,h})\|_{\mathbf{V}(K)\times Q(K)} + h_K^{1/2}\|\boldsymbol{\lambda}-\boldsymbol{\lambda}_H\|_{0,\partial K},$$

and then the right-hand side is fully computable if the exact solution is available.

5 Numerical experiments

This section presents numerical experiments, using three different examples, to demonstrate the reliability and efficiency of our a posteriori error estimator. We validate an adaptive refinement algorithm procedure based on refining faces, which keeps the topology of the first-level mesh untouched.

For all $F \in \mathscr{E}_H$, we define:

$$\eta_F := \left\{\sum_{\tilde{F}\in\mathscr{T}_{\tilde{H}}(F)} \eta_{1,\tilde{F}}^2\right\}^{1/2} + \sum_{K\in\omega_F}\eta_{2,K}, \quad \text{with} \quad \eta_{1,\tilde{F}} := \frac{\|\boldsymbol{R}_F\|_{0,\tilde{F}}}{H_F^{1/2}}. \tag{52}$$

Thus, the adaptive algorithm that uses (52) is the following:

Algorithm 1 Adaptivity by faces procedure.

Require: $\theta \in (0, 1)$ and a coarse first-level mesh $\mathscr{T}_H$.

1: Solve the discrete problems (24) and (28)–(29) on the current mesh.

2: For each $F \in \mathscr{E}_H$, compute the local error indicator η_F in (52).

3: Given $F \in \mathscr{E}_H$ such that $\eta_F \geq \theta \max_{F \in \mathscr{E}_H} \eta_F$, refine $\tilde{F} \in \mathscr{T}_{\tilde{H}}(F)$ such that $\eta_{1,\tilde{F}} = \max_{\mathscr{T}_{\tilde{H}}(F)} \eta_{1,\tilde{F}}$, and if $\eta_{1,F} < \sum_{K \in \omega_F} \eta_{2,K}$ also refine the second-level meshes $\mathscr{T}_h^K$ for $K \in \omega_F$.

4: If the stop criterion is not satisfied, repeat the algorithm.

Using the procedure given in the Algorithm 1, the first-level mesh does not change, and only the local problem associated with elements "touched" by the estimator needs to be revisited. Thereby, only a few extra entries must be computed and assembled into the global system in each adaption step. This algorithm is particularly attractive for use in real three-dimensional problems since it dramatically decreases the computational cost involved in the adaptive procedure and avoids three-dimensional global re-meshing.

5.1 A smooth solution

The domain is $\Omega := (0, 1) \times (0, 1)$, $\nu := 1$, $\gamma := 1$, $\boldsymbol{\alpha} := \left(\frac{1}{\sqrt{2}}, \frac{1}{\sqrt{2}}\right)$, $\boldsymbol{f}$ and the boundary conditions are chosen such that the exact solution is given by:

$$u_1(x, y) := -256x^2(x-1)^2 y(y-1)(2y-1), \quad u_2(x, y) := -u_1(y, x), \quad p(x, y) := (x-y)^6 - \frac{1}{28}.$$

Using a uniform refinement in the first-level mesh, with one element at the second-level mesh, and polynomial degrees, on the faces, $\boldsymbol{\Lambda}_l$, $l = 0, 1, 2$, Table 1 shows the convergence of the a posteriori error estimators η_1, η_2 and the effectivity index, E defined by:

$$E := \frac{\eta}{\|(\boldsymbol{u} - \boldsymbol{u}_{H,h}, p - p_{H,h})\|_{\mathbf{V}\times Q}},$$

where η is given in (34). First, we set viscosity $\nu = 1$ and observe that the effectivity index stays close to 1 in all scenarios. From the perspective of the impact of the one- and second-level estimators in the effectivity index, we see that both are relevant when the mesh is coarse, and l is low. Otherwise, the second-level estimator η_2 becomes one order of magnitude higher compared with its one-level counterpart η_1. This corresponds to an expected behaviour as one adopted one-element sub-meshes in those numerical simulations. Indeed, if one uses refined sub-meshes, their importance switch (see [11, Section 5]).

Figures 2, 3, and 4 illustrate the convergence aspects for the MHM method. We observe the expected convergence orders $\mathscr{O}(H^{l+1})$, $l = 0, 1, 2$, in the $\|\cdot\|_{\mathbf{V}\times Q}$ norm for the exact error, as well as for the error estimator η.

Table 1 Exact error, a posteriori error estimators, and effectivity index for $\nu = 1$, $\boldsymbol{u}_{H,h} \in \mathbb{P}_3^2$, $p_{H,h} \in \mathbb{P}_3$, and $\boldsymbol{\lambda}_{H,h} \in \boldsymbol{\Lambda}_l$, $l = 0, 1, 2$

l	H	$\\|(\boldsymbol{u} - \boldsymbol{u}_{H,h}, p - p_{H,h})\\|_{\mathbf{V}\times Q}$	η_1	η_2	E
	0.25	0.8472405×10^{-1}	0.6778663×10^{-2}	0.9707391×10^{-1}	1.225775
	0.125	0.9915863×10^{-2}	0.9197585×10^{-3}	0.1084051×10^{-1}	1.186005
2	0.0625	0.1208512×10^{-2}	0.1213830×10^{-3}	0.1300599×10^{-2}	1.176639
	0.03125	0.1497330×10^{-3}	0.1572163×10^{-4}	0.1604838×10^{-3}	1.176798
	0.015625	0.1865182×10^{-4}	0.2006059×10^{-5}	0.1997001×10^{-4}	1.178227
	0.25	0.3228006	0.8209395×10^{-1}	0.3214077	1.250003
	0.125	0.7916980×10^{-1}	0.2200528×10^{-1}	0.8110115×10^{-1}	1.302346
1	0.0625	0.1960050×10^{-1}	0.5795234×10^{-2}	0.1957939×10^{-2}	1.294591
	0.03125	0.4904711×10^{-2}	0.1499087×10^{-2}	0.4759787×10^{-2}	1.276094
	0.015625	0.1228986×10^{-2}	0.3820426×10^{-3}	0.1169730×10^{-2}	1.262644
	0.25	0.2585779×10	0.1103852×10	0.1311145×10	0.9339536
	0.125	0.1314891×10	0.6038400	0.6121682×10	0.9247977
0	0.0625	0.6590541	0.3207728	0.3056109	0.9504282
	0.03125	0.3296247	0.1652682	0.1529013	0.9652478
	0.015625	0.1648197	0.8381923×10^{-1}	0.7646742×10^{-1}	0.9724971

Next, we diminish viscosity values to $\nu = 10^{-2}$ and $\nu = 10^{-4}$, and observe that the effectivity index changes as the ν decreases. The results are shown in Tables 2 and 3. Such a behaviour indicates that the constants are not robust concerning the physical parameters in the advective dominate regime as usual. Regarding how the one- and second-level estimators impact the effectivity index, we see a different scenario to the case $\nu = 1$. Indeed, we observed a prevalence of the first level estimator η_1 over the second-level contribution η_2 for all l and mesh refinement cases.

In the context of $\nu = 10^{-2}$, we revisite the convergence aspects for the MHM method in Figs. 5, 6, and 7. Again, we observe the expected convergence orders $\mathcal{O}(H^{l+1})$, $l = 0, 1, 2$, in the $\\| \cdot \\|_{\mathbf{V}\times Q}$ norm for the exact error and for the error estimator η.

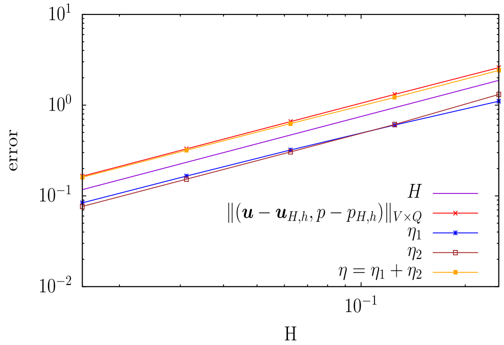

Fig. 2 Estimated and exact error curves for $\nu = 1$, $\boldsymbol{u}_{H,h} \in \mathbb{P}_3^2$, $p_{H,h} \in \mathbb{P}_3$, and $\boldsymbol{\lambda}_{H,h} \in \boldsymbol{\Lambda}_0$

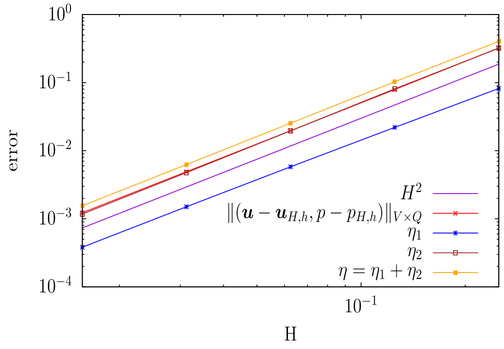

Fig. 3 Estimated and exact error curves for $\nu = 1$, $\boldsymbol{u}_{H,h} \in \mathbb{P}_3^2$, $p_{H,h} \in \mathbb{P}_3$, and $\boldsymbol{\lambda}_{H,h} \in \boldsymbol{\Lambda}_1$

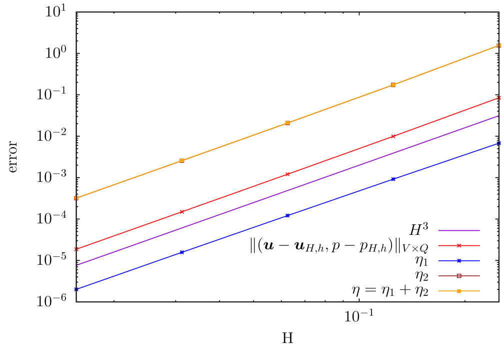

Fig. 4 Estimated and exact error curves for $\nu = 1$, $\boldsymbol{u}_{H,h} \in \mathbb{P}_3^2$, $p_{H,h} \in \mathbb{P}_3$, and $\boldsymbol{\lambda}_{H,h} \in \boldsymbol{\Lambda}_2$

Table 2 Exact error, a posteriori error estimators, and effectivity index for $\nu = 10^{-2}$, $\boldsymbol{u}_{H,h} \in \mathbb{P}_3^2$, $p_{H,h} \in \mathbb{P}_3$, and $\boldsymbol{\lambda}_{H,h} \in \boldsymbol{\Lambda}_l$, $l = 0, 1, 2$

l	H	$\|(\boldsymbol{u} - \boldsymbol{u}_{H,h}, p - p_{H,h})\|_{\mathbf{V}\times Q}$	η_1	η_2	E
	0.25	0.9219341×10^{-1}	0.1381117×10^{-1}	0.2259165×10^{-2}	0.1743111
	0.125	0.1351087×10^{-1}	0.2282492×10^{-2}	0.2642712×10^{-3}	0.1884973
2	0.0625	0.1807365×10^{-2}	0.3241413×10^{-3}	0.3199841×10^{-4}	0.1970491
	0.03125	0.2319275×10^{-3}	0.4286884×10^{-4}	0.3955605×10^{-5}	0.2018926
	0.015625	0.2924521×10^{-4}	0.5481446×10^{-5}	0.4930700×10^{-6}	0.2042904
	0.25	0.1318692×10^{1}	0.3744764	0.5586192×10^{-1}	0.3263372
	0.125	0.4516195	0.1371993	0.1269113×10^{-1}	0.3318953
1	0.0625	0.1292889	0.4146891×10^{-1}	0.2813878×10^{-2}	0.3425105
	0.03125	0.3409020×10^{-1}	0.1125197×10^{-1}	0.6678104×10^{-3}	0.3496542
	0.015625	0.8695222×10^{-2}	0.2902015×10^{-2}	0.1644081×10^{-3}	0.3526561
	0.25	0.6843741×10^{1}	0.2697528×10^{1}	0.9616601	0.5346766
	0.125	0.5138595×10^{1}	0.2314727×10^{1}	0.3164794	0.5120479
0	0.0625	0.3192640×10^{1}	0.1603597×10^{1}	0.8086800×10^{-1}	0.5276087
	0.03125	0.1764631×10^{1}	0.9419820	0.2496842×10^{-1}	0.5479618
	0.015625	0.9141707	0.5011848	0.1050770×10^{-1}	0.5597341

Table 3 Exact error, a posteriori error estimators, and effectivity index for $\nu = 10^{-4}$, $\boldsymbol{u}_{H,h} \in \mathbb{P}_3^2$, $p_{H,h} \in \mathbb{P}_3$, and $\boldsymbol{\lambda}_{H,h} \in \boldsymbol{\Lambda}_l$, $l = 0, 1, 2$

l	H	$\\|(\boldsymbol{u}-\boldsymbol{u}_{H,h}, p-p_{H,h})\\|_{\mathbf{V}\times Q}$	η_1	η_2	E
	0.25	0.4022419	0.3631610×10^{-1}	0.1716682×10^{-2}	0.0945520
	0.125	0.1144633	0.1169604×10^{-1}	0.2116221×10^{-3}	0.1040304
2	0.0625	0.2087342×10^{-1}	0.2525211×10^{-2}	0.4145032×10^{-4}	0.1229632
	0.03125	0.3664576×10^{-2}	0.5554220×10^{-3}	0.1542330×10^{-4}	0.1557739
	0.015625	0.6568818×10^{-3}	0.1138560×10^{-3}	0.5285791×10^{-5}	0.1813747
	0.25	7.862317	1.791742	0.1146125	0.2424673
	0.125	4.777998	1.126343	0.3938183×10^{-1}	0.2439777
1	0.0625	2.208454	0.538928	0.1392532×10^{-1}	0.2503351
	0.03125	0.8120287	0.2109413	0.7782620×10^{-2}	0.2693549
	0.015625	0.2793878	0.7671757×10^{-1}	0.4562518×10^{-2}	0.2909221
	0.25	0.3147448×10^{2}	6.048800	1.327762	0.2343664
	0.125	0.3264509×10^{2}	6.472617	0.7475223	0.2211708
0	0.0625	0.2511912×10^{2}	5.629570	0.5023346	0.2441131
	0.03125	0.1703080×10^{2}	4.456101	0.7500895	0.3056927
	0.015625	0.1302838×10^{2}	3.966013	1.082794	0.3875238

5.2 Boundary layer solution

We consider the domain $\Omega := (0,1) \times (0,1)$, $\nu := 10^{-2}$, $\gamma = 1$, $\boldsymbol{\alpha} := \left(\frac{1}{\sqrt{2}}, \frac{1}{\sqrt{2}}\right)$, $\boldsymbol{f}$ and the boundary conditions are chosen such that the exact solution is given by:

$$u_1(x,y) := y - \frac{1-e^{y/\nu}}{1-e^{1/\nu}}, \quad u_2(x,y) := x - \frac{1-e^{x/\nu}}{1-e^{1/\nu}}, \quad p(x,y) := (x-y)^8 - \frac{1}{45}.$$

The solutions u_1 and u_2 exhibit boundary layers at $y = 1$ and $x = 1$, respectively. A structured mesh of 64 elements in the first level is used. In all the calculations $\boldsymbol{u}_{H,h} \in \mathbb{P}_3^2$, $p_{H,h} \in \mathbb{P}_3$, and $\boldsymbol{\lambda}_{H,h} \in \boldsymbol{\Lambda}_1$. Figure 8 shows the adaptivity procedure by faces (Algorithm 1) and isovalues of vertical component of velocity. The red dots

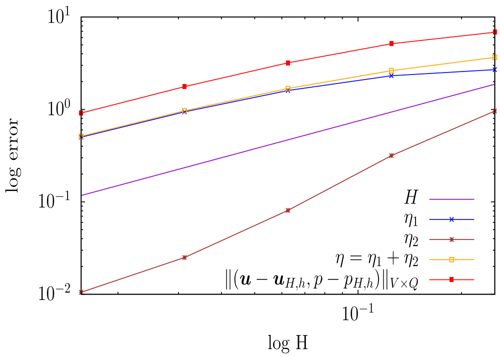

Fig. 5 Estimated and exact error curves for $\nu = 10^{-2}$, $\boldsymbol{u}_{H,h} \in \mathbb{P}_3^2$, $p_{H,h} \in \mathbb{P}_3$, and $\boldsymbol{\lambda}_{H,h} \in \boldsymbol{\Lambda}_0$

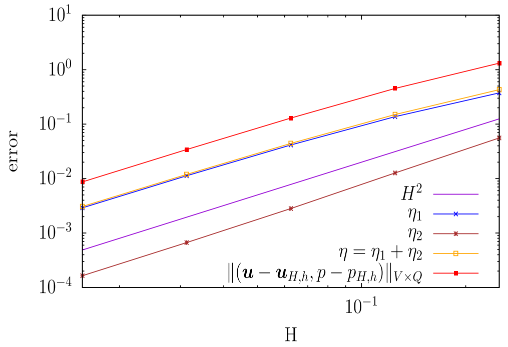

Fig. 6 Estimated and exact error curves for $\nu = 10^{-2}$, $\boldsymbol{u}_{H,h} \in \mathbb{P}_3^2$, $p_{H,h} \in \mathbb{P}_3$, and $\boldsymbol{\lambda}_{H,h} \in \boldsymbol{\Lambda}_1$

in the mesh of the first level represent faces where more basis functions have been added to improve the approximation of $\boldsymbol{\Lambda}_1$. In the second level, a structured mesh, which coincides with $\mathscr{T}_{\tilde{H}}(F)$, $F \in \partial K$, $K \in \mathscr{T}_H$, is used.

The adaptive algorithm associated with the multiscale estimator may induce an anisotropic adaptation on second-level mesh due to the sharp boundary layers. Also observe that the solution is improved without changing the topology of the coarse first-level mesh.

5.3 Solution with an inner layer

Let $\Omega := (0,1)^2$, $\nu := 10^{-3}$, $\gamma := 0$ and $\boldsymbol{\alpha} := (1,0)$. We consider $\phi(x,y) := x^2(1-x)^2y^2(1-y)^2\,(1-\tanh(75-150x))$, $\boldsymbol{f}$ and the boundary conditions are chosen such that the exact solution is:

$$\boldsymbol{u} := \boldsymbol{curl}\,\phi = \left(\frac{\partial \phi}{\partial y}, -\frac{\partial \phi}{\partial x}\right), \qquad p := (x-y)^6 - \frac{1}{28}.$$

This solution presents an inner layer around $x = 1/2$. For this case, we choose a first-level mesh which is not aligned to advection. In Fig. 9, we present the adaptive procedure by faces for this test case. The red dots near the inner layer indicate the faces where basis functions were added to the subspace $\boldsymbol{\Lambda}_1$. In the second-level a structured mesh, which coincides with $\mathscr{T}_{\tilde{H}}(F)$, $F \in \partial K$, $K \in \mathscr{T}_H$, is used.

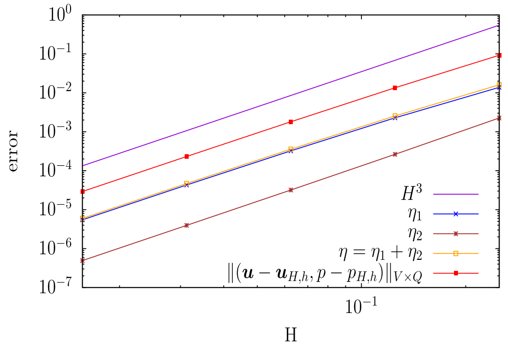

Fig. 7 Estimated and exact error curves for $\nu = 10^{-2}$, $\boldsymbol{u}_{H,h} \in \mathbb{P}_3^2$, $p_{H,h} \in \mathbb{P}_3$, and $\boldsymbol{\lambda}_{H,h} \in \boldsymbol{\Lambda}_2$

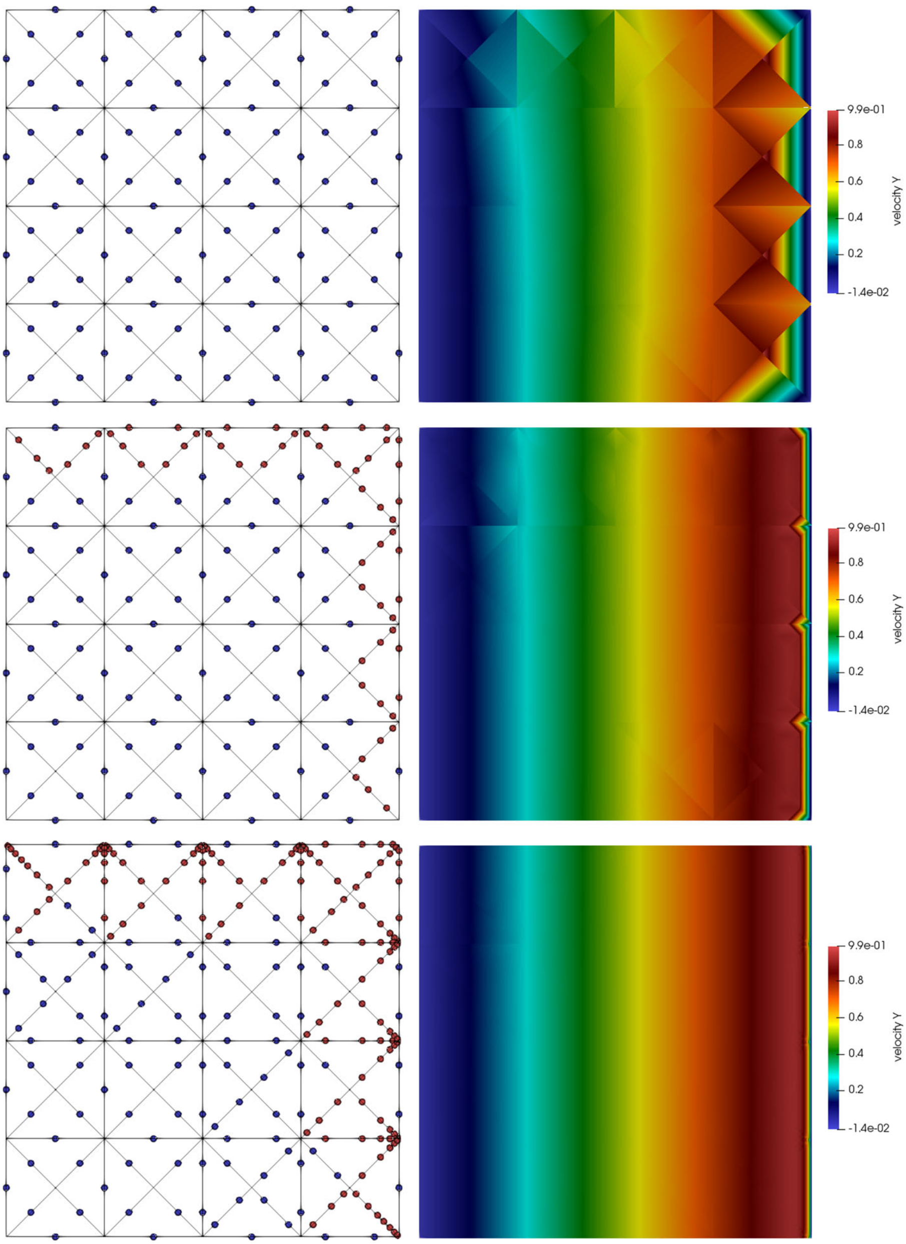

Fig. 8 Adaptivity procedure by faces (left) and isovalues of vertical component (right). Here $\boldsymbol{u}_{H,h} \in \mathbb{P}_3^2$, $p_{H,h} \in \mathbb{P}_3$, and $\boldsymbol{\lambda}_{H,h} \in \boldsymbol{\Lambda}_1$

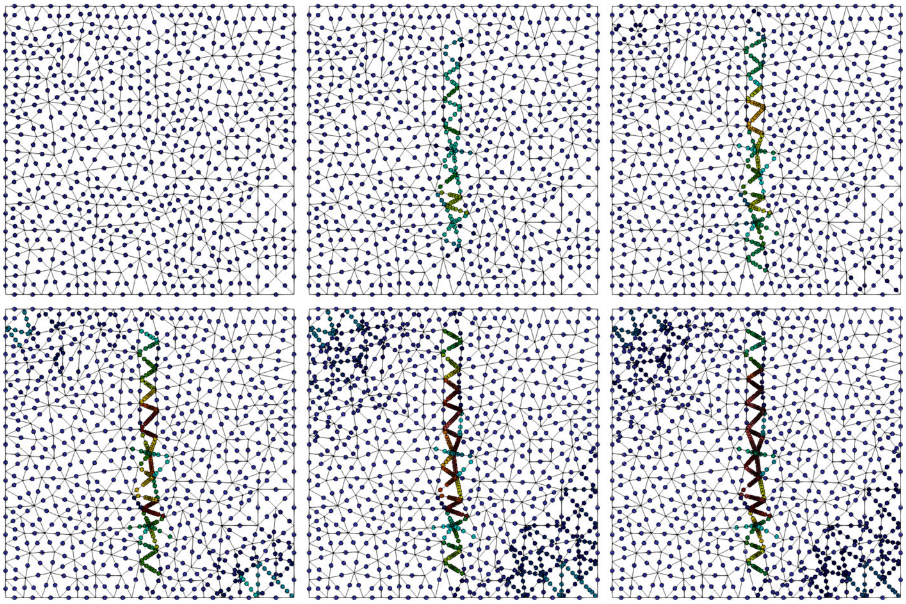

Fig. 9 Adaptivity procedure by faces at iterations 0, 5, 10, 20, 30, and 50 (from top-right to bottom-left)

Figure 10 shows the isolines of the absolute value of the velocity at iterations 0, 5, 10, 20, 30, and 50 of the adaptive procedure. Here we set $\boldsymbol{u}_{H,h} \in \mathbb{P}_3^2$, $p_{H,h} \in \mathbb{P}_3$ and $\boldsymbol{\lambda}_{H,h} \in \boldsymbol{\Lambda}_1$. Observe the great improvements in the solution by just adding a few extra dof at the right location induced by the multiscale estimator.

The improvements to the computed solution in the final adapted mesh can be seen in Fig. 11, where we show the profile of the components of the velocity near the inner layer in horizontal cuts. We notice that the adapted scheme captures the inner layer correctly by comparing it with the exact solution.

6 Conclusions

This work proposed a novel MHM method to the Oseen equations based on previous works for the Stokes model [9] and for the advection-diffusion equation [39]. Owing to the MHM's structure, we also introduced and analysed a new residual a posteriori error estimator for which we showed that local efficiency and reliability hold with respect to natural norms. The estimator is multilevel, and then it is able to account for different scales, and then handle the solutions of singularly perturbed problems as the ones in the Oseen equations under advective or reactive regimes. From theoretical view-point, the dependence of constants (in the equivalence estimates) with respect to the physical parameters as well as to the degree of polynomial interpolation on faces deserves further investigation. Numerical verifications performed in this work pointed towards a mild dependence of those constants in terms of polynomial degree. However, a stronger dependency appeared with respect to the physical

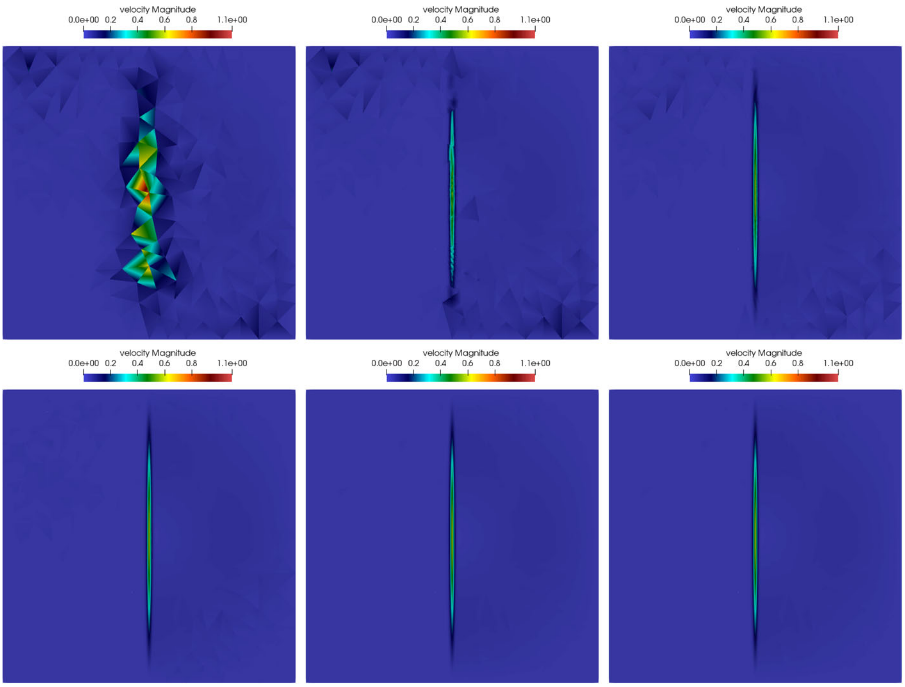

Fig. 10 Isolines of the absolute value of the velocity field at iterations 0, 5, 10, 20, 30, and 50. Here $\boldsymbol{u}_{H,h} \in \mathbb{P}_3^2$, $p_{H,h} \in \mathbb{P}_3$, and $\boldsymbol{\lambda}_{H,h} \in \boldsymbol{\Lambda}_1$

parameters as it is usually the case in advective-dominate problems. The precise characterisation of those dependencies stays an open problem. The natural extension of the proposed methodology to the non-linear Navier-Stokes equations is currently under investigation.

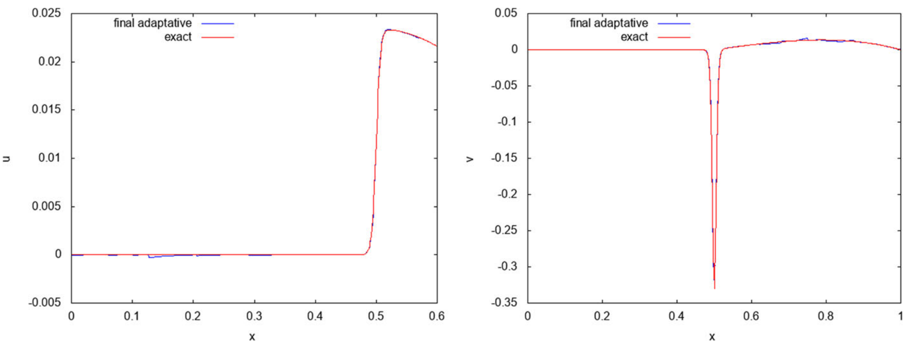

Fig. 11 Tangential velocity profiles at $y = 0.25$ (left) and normal velocity profiles at $y = 0.5$ in iteration final of the adaptive process. Here $\boldsymbol{u}_{H,h} \in \mathbb{P}_3^2$ and $\boldsymbol{\lambda}_{H,h} \in \boldsymbol{\Lambda}_1$

Funding The first author was partially supported by ANID-Chile through the project Centro de Modelamiento Matemático (AFB170001) of the PIA Program: Concurso Apoyo a Centros Científicos y Tecnológicos de Excelencia con Financiamiento Basal, and Universidad de Concepción through project VRID 219.013.046-INV. The second author was partially supported by CONICYT-Chile through scholarship PCHA/Doctorado Nacional. The third author was partially supported by Dirección de Investigación of the Universidad Católica de la Santísima Concepción through project DIREG 01/2020. The fourth author was partially supported by CNPq/Brazil No. 301576/2013-0 and by CAPES/Brazil No. 88881.143295/2017-01 under the PHOTOM Project.

References

1. Abdulle, A., Nonnenmacher, A.: A posteriori error estimates in quantities of interest for the finite element heterogeneous multiscale method. Numer. Methods Partial Differential Equations **29**(5), 1629–1656 (2013). https://doi.org/10.1002/num.21769
2. Agmon, S.: Lectures on Elliptic Boundary Problems. AMS Chelsea Publishing, Providence (2010). https://doi.org/10.1090/chel/369
3. Ahmed, N., Chacón, T., John, V., Rubino, S.: A review of variational multiscale methods for the simulation of turbulent incompressible flows. Arch. Comput. Methods Eng. **24**(1), 115–164 (2017). https://doi.org/10.1007/s11831-015-9161-0
4. Ainsworth, M., Oden, J.T.: A posteriori error estimation in finite element analysis. Pure and Applied Mathematics (New York). Wiley-Interscience [John Wiley & Sons], New York (2000). https://doi.org/10.1002/9781118032824
5. Araya, R., Barrenechea, G.R., Poza, A.H., Valentin, F.: Convergence analysis of a residual local projection finite element method for the Navier-Stokes equations. SIAM J. Numer. Anal. **50**(2), 669–699 (2012). https://doi.org/10.1137/110829283
6. Araya, R., Barrenechea, G.R., Valentin, F.: Stabilized finite element methods based on multiscale enrichment for the Stokes problem. SIAM J. Numer. Anal. **44**(1), 322–348 (2006)
7. Araya, R., Bertoglio, C., Cárcamo, C., Poza, A.H., Valentin, F.: Multiscale hybrid-mixed method for the Oseen equation. In preparation (2021)
8. Araya, R., Harder, C., Paredes, D., Valentin, F.: Multiscale hybrid-mixed method. SIAM J. Numer. Anal. **51**(6), 3505–3531 (2013). https://doi.org/10.1137/120888223
9. Araya, R., Harder, C., Poza, A.H., Valentin, F.: Multiscale hybrid-mixed method for the Stokes and Brinkman equations - The method. Comput. Methods Appl. Mech. Engrg. **324**(1), 172–197 (2017). https://doi.org/10.1016/j.cma.2017.05.027
10. Araya, R., Poza, A.H., Valentin, F.: An adaptive residual local projection finite element method for the Navier–Stokes equations. Adv. Comput. Math. **40**(5), 1093–1119 (2014). https://doi.org/10.1007/s10444-014-9343-6
11. Araya, R., Rebolledo, R., Valentin, F.: On a multiscale a posteriori error estimator for the Stokes and Brinkman equations. IMA J. Numer Anal. https://doi.org/10.1093/imanum/drz053 (2019)
12. Arbogast, T., Pencheva, G., Wheeler, M.F., Yotov, I.: A multiscale mortar mixed finite element method. Multiscale Model Simul. **6**(1), 319–346 (2007). https://doi.org/10.1137/060662587
13. Babuska, I., Osborn, E.: Generalized finite element methods: their performance and their relation to mixed methods. SIAM J. Num. Anal. **20**(3), 510–536 (1983)
14. Baiges, J., Codina, R.: Variational multiscale error estimators for solid mechanics adaptive simulations: an orthogonal subgrid scale approach. Comput. Methods Appl. Mech. Engrg. **325**, 37–55 (2017). https://doi.org/10.1016/j.cma.2017.07.008
15. Barrenechea, G., Fernández, M., Vidal, C.: A stabilized finite element method for the Oseen equation with dominating reaction. Research Report RR-5213, INRIA. https://hal.inria.fr/inria-00070780 (2004)
16. Barrenechea, G.R., Franca, L.P., Valentin, F.: A Petrov-Galerkin enriched method: a mass conservative finite element method for the Darcy equation. Comput. Methods Appl. Mech. Engrg. **196**(21-24), 2449–2464 (2007). https://doi.org/10.1016/j.cma.2007.01.004
17. Barrenechea, G.R., Valentin, F.: A residual local projection method for the Oseen equation. Comput. Methods Appl. Mech. Engrg. **199**(29-32), 1906–1921 (2010). https://doi.org/10.1016/j.cma.2010.01.014

18. Bi, C., Wang, C., Lin, Y.: Two-grid finite element method and its a posteriori error estimates for a nonmonotone quasilinear elliptic problem under minimal regularity of data. Comput. Math. Appl. **76**(1), 98–112 (2018). https://doi.org/10.1016/j.camwa.2018.04.006
19. Brenner, S.C., Scott, L.R. The Mathematical Theory of Finite Element Methods. Texts in Applied Mathematics, 3rd edn., vol. 15. Springer, New York (2008). https://doi.org/10.1007/978-0-387-75934-0
20. Cesmelioglu, A., Cockburn, B., Nguyen, N.C., Peraire, J.: Analysis of HDG methods for Oseen equations. J. Sci. Comput. **55**(2), 392–431 (2013). https://doi.org/10.1007/s10915-012-9639-y
21. Chamoin, L., Legoll, F.: A posteriori error estimation and adaptive strategy for the control of msFEM computations. Comput. Methods Appl. Mech. Engrg. **336**, 1–38 (2018). https://doi.org/10.1016/j.cma.2018.02.016
22. Ciarlet, P.G.: The Finite Element Method for Elliptic Problems. Vol. 40. Society for Industrial and Applied Mathematics (SIAM), Philadelphia (2002)
23. Clément, P.: Approximation by finite element functions using local regularization. R.A.I.R.O Anal. Numer. **9**(R-2), 77–84 (1975)
24. Cockburn, B., Gopalakrishnan, J., Lazarov, R.: Unified hybridization of discontinuous Galerkin, mixed, and continuous Galerkin methods for second order elliptic problems. SIAM J. Numer. Anal. **47**(2), 1319–1365 (2009). https://doi.org/10.1137/070706616
25. Davidson, P.A. Turbulence. An Introduction for Scientists and Engineers, 2nd edn. Oxford University Press, Oxford (2015). https://doi.org/10.1093/acprof:oso/9780198722588.001.0001
26. Durán, R.: An elementary proof of the continuity from $L^2_0(\Omega)$ to $H^1_0(\Omega)$ of Bogovskii's right inverse of the divergence. Rev. Un. Mat. Argentina **53**(2), 59–78 (2012)
27. E, W., Engquist, B., Li, X., Ren, W., Vanden-Eijnden, E.: Heterogeneous multiscale methods: a review. Commun. Comput. Phys. **2**(3), 367–450 (2007)
28. Efendiev, Y., Galvis, J., Hou, T.Y.: Generalized multiscale finite element methods (GMsFEM). J. Comput. Phys. **251**, 116–135 (2013). https://doi.org/10.1016/j.jcp.2013.04.045
29. Ern, A., Guermond, J.L.: Theory and Practice of Finite Elements. Applied Mathematical Sciences, vol. 159. Springer, New York (2004). https://doi.org/10.1007/978-1-4757-4355-5
30. Ervin, V., Layton, W., Maubach, J.: A posteriori error estimators for a two-level finite element method for the Navier-Stokes equations. Numer. Methods Partial Differential Equations **12**(3), 333–346 (1996). https://doi.org/10.1002/(SICI)1098-2426(199605)12:3⟨333::AID-NUM4⟩3.0.CO;2-P
31. Farhat, C., Harari, I., Franca, L.P.: The discontinuous enrichment method. Comput. Methods Appl. Mech. Engrg. **190**(48), 6455–6479 (2001). https://doi.org/10.1016/S0045-7825(01)00232-8
32. Ferziger, J.H., Perić, M., Street, R.L. Computational Methods for Fluid Dynamics, 4th edn. Springer, Cham (2020). https://doi.org/10.1007/978-3-319-99693-6
33. Foias, C., Manley, O., Rosa, R., Temam, R.: Navier-Stokes Equations and Turbulence. Encyclopedia of Mathematics and its Applications, vol. 83. Cambridge University Press, Cambridge (2001). https://doi.org/10.1017/CBO9780511546754
34. Franca, L.P., Harder, C., Valentin, F.: On a residual local projection method for the Darcy equation. C. R. Math. Acad. Sci. Paris **347**(17-18), 1105–1110 (2009). https://doi.org/10.1016/j.crma.2009.06.016
35. Franca, L.P., Madureira, A.L.: Element diameter free stability parameters for stabilized methods applied to fluids. Comput. Methods Appl. Mech. Engrg. **105**(3), 395–403 (1993). https://doi.org/10.1016/0045-7825(93)90065-6
36. Franca, L.P., Madureira, A.L., Valentin, F.: Towards multiscale functions: enriching finite element spaces with local but not bubble-like functions. Comput. Methods Appl. Mech. Engrg. **194**(27-29), 3006–3021 (2005). https://doi.org/10.1016/j.cma.2004.07.029
37. Harder, C., Madureira, A.L., Valentin, F.: A hybrid-mixed method for elasticity. ESAIM Math. Model. Numer. Anal. **50**(2), 311–336 (2016). https://doi.org/10.1051/m2an/2015046
38. Harder, C., Paredes, D., Valentin, F.: A family of multiscale hybrid-mixed finite element methods for the Darcy equation with rough coefficients. J. Comput. Phys. **245**, 107–130 (2013). https://doi.org/10.1016/j.jcp.2013.03.019
39. Harder, C., Paredes, D., Valentin, F.: On a multiscale hybrid-mixed method for advective-reactive dominated problems with heterogenous coefficients. SIAM Multiscale Model. and Simul. **13**(2), 491–518 (2015). https://doi.org/10.1137/130938499
40. Henning, P., Målqvist, A., Peterseim, D.: A localized orthogonal decomposition method for semi-linear elliptic problems. ESAIM Math. Model. Numer. Anal. **48**(5), 1331–1349 (2014). https://doi.org/10.1051/m2an/2013141

41. Henning, P., Ohlberger, M.: A-posteriori error estimate for a heterogeneous multiscale approximation of advection-diffusion problems with large expected drift. Discrete Contin. Dyn. Syst. Ser. S **9**(5), 1393–1420 (2016). https://doi.org/10.3934/dcdss.2016056
42. Hou, T.Y., Wu, X.H.: A multiscale finite element method for elliptic problems in composite materials and porous media. J. Comput. Phys. **134**(1), 169–189 (1997). https://doi.org/10.1006/jcph.1997.5682
43. Hou, T.Y., Wu, X.H., Cai, Z.: Convergence of a multiscale finite element method for elliptic problems with rapidly oscillating coefficients. Math. Comp. **68**(227), 913–943 (1999). https://doi.org/10.1090/S0025-5718-99-01077-7
44. Irisarri, D., Hauke, G.: A posteriori pointwise error computation for 2-D transport equations based on the variational multiscale method. Comput. Methods Appl. Mech. Engrg. **311**, 648–670 (2016). https://doi.org/10.1016/j.cma.2016.09.001
45. John, V.: Residual a posteriori error estimates for two-level finite element methods for the Navier-Stokes equations. Appl. Numer. Math. **37**(4), 503–518 (2001). https://doi.org/10.1016/S0168-9274(00)00058-1
46. John, V.: Finite Element Methods for Incompressible Flow Problems. Springer Series in Computational Mathematics, vol. 51. Springer, Cham (2016). https://doi.org/10.1007/978-3-319-45750-5
47. Ohlberger, M.: A posteriori error estimates for the heterogeneous multiscale finite element method for elliptic homogenization problems. Multiscale Model Simul. **4**(1), 88–114 (2005). https://doi.org/10.1137/040605229
48. Paredes, D., Valentin, F., Versieux, H.M.: On the robustness of multiscale hybrid-mixed methods. Math. Comp. **86**(304), 525–548 (2017). https://doi.org/10.1090/mcom/3108
49. Pencheva, G.V., Vohralík, M., Wheeler, M.F., Wildey, T.: Robust a posteriori error control and adaptivity for multiscale, multinumerics, and mortar coupling. SIAM J. Numer. Anal. **51**(1), 526–554 (2013). https://doi.org/10.1137/110839047
50. Pope, S.B.: Turbulent Flows. Cambridge University Press. (2000). https://doi.org/10.1017/CBO9780511840531675
51. Raviart, P.A., Thomas, J.M.: Primal hybrid finite element methods for 2nd order elliptic equations. Math. Comp. **31**(138), 391–413 (1977). https://doi.org/10.2307/2006423
52. Ren, C., Ma, Y.: Residual a posteriori error estimate of a new two-level method for steady Navier-Stokes equations. J. Syst. Sci. Complex. **19**(4), 478–490 (2006). https://doi.org/10.1007/s11424-006-0478-5
53. Tavener, S., Wildey, T.: Adjoint based a posteriori analysis of multiscale mortar discretizations with multinumerics. SIAM J. Sci. Comput. **35**(6), A2621–A2642 (2013). https://doi.org/10.1137/12089973X
54. Xu, J.: Two-grid discretization techniques for linear and nonlinear PDEs. SIAM J. Numer. Anal. **33**(5), 1759–1777 (1996). https://doi.org/10.1137/S0036142992232949
55. Zhang, Y.Z., Hou, Y.R., Wei, H.B.: Residual a posteriori error estimate of two level finite element method for natural convection problem. Gongcheng Shuxue Xuebao **32**(1), 116–130 (2015)

Publisher's note Springer Nature remains neutral with regard to jurisdictional claims in published maps and institutional affiliations.